Resource selection and relative abundance of Swainson's Warbler (*Limnothlypis swainsonii*) in the Appalachian Mountains on Cherokee National Forest, Tennessee

A Thesis Presented for the

Master of Science

Degree

The University of Tennessee, Knoxville

Dawson William Rader

December 2024

Dedication

This thesis is dedicated to Mana, thank you for your unwavering support. It is one of my greatest regrets that you weren't here to see this final product.

Acknowledgements

I would not be submitting this thesis without the people who have supported me through this journey. First, I must thank my family and partner; mom, dad, Nona, grandaddy, Mana, Audrey, and Nora, who have offered me unending support and encouragement throughout this process. You all never doubted me, and always fought to build me back up when I was feeling defeated or overwhelmed by this project.

A special thanks must also be extended to my advisor, Dr. David Buehler. You guided me through this journey, all the while honing my skills and preparing me for the world of wildlife science which lies ahead. None of this would have been possible without your input, edits and expertise, and for that I am immensely grateful. I also have to thank my wonderful committee members, Dr. Jeff Atkins, whose knowledge and assistance allowed me to utilize LiDAR data which otherwise I would have never been able to accomplish, Dr. D.J. McNeil, who was always on call to patiently explain and assist with R code and statistics, and Dr. David Buckley, who always ensured that I was always thinking about how my work and findings could contribute to forest ecology and wildlife science as a whole.

The fieldwork for this project was intensive to say the least. Thank you to my technician, Carly Naundorff, who helped me to complete two long, brutal seasons of vegetation sampling. The Cherokee National Forest forestry interns assisted in vegetation sampling as well. Thank you all, your efforts and tree I.D. expertise were integral to me staying on schedule each season.

And lastly, I must thank TWRA, USFS, the University of Tennessee School of Natural Resources, and the Tennessee Ornithological Society, who together provided funding, housing and transportation required to complete this study

One last time, Thank you all!

Abstract

The Swainson's Warbler is a Nearctic-Neotropical songbird that breeds across the southeastern United States in two main, geographically-disjunct regions: the Southeastern Coastal Plains and the Appalachian Mountains. In Tennessee, the Swainson's Warbler is a species of conservation concern, but the breeding territory characteristics and distribution of this species in the Appalachian Mountain portion of its range remain largely unstudied. Our objectives for this study were to 1. identify vegetation metrics that drive Swainson's Warbler territory selection, 2. model Swainson's Warbler abundance on the 88,000-ha, southern ranger districts of the Cherokee National Forest, 3. inform Swainson's Warbler monitoring and management in the southern Appalachian Mountains. We conducted Swainson's Warbler 5-min, point-count surveys in 2022 and 2023 along 99 km of secondary roads on the forest and located a total of 125 unique individuals, an average of 0.59 territories/km. We randomly selected 60 territory and 60 absence plots where we collected on-the-ground and LIDAR-derived vegetation metrics and analyzed all metrics in a resource-selection framework via logistic regression. The best-supported model contained percent understory ($\beta = 7.34 \pm 1.45$ SE, 95% CI [4.28, 10.4]) and visual obstruction ($\beta = 0.56 \pm 0.18$ SE, 95% CI [0.18, 0.95]). Additionally, we used multinomial N-mixture models with remotely-sensed covariates to determine which covariates best predicted Swainson's Warbler relative abundance. The best-performing model included slope, mean outer canopy height, topographic wetness index, and percent of first returns below 1 m. We estimated there was 3,520 ha of potential Swainson's Warbler habitat on the southern ranger districts of Cherokee National Forest, 55% of which was within 200 m of roads. Thus, 5-min point-count surveys along roadsides could effectively monitor the Swainson's Warbler

population on the southern ranger districts of the Cherokee National Forest. An estimated 26% of potential habitat was located within 30 m of streams and was thus affected by current streamside management zone guidelines. This study documented the largest known breeding population of Swainson's Warblers in the Appalachian Mountains. Knowledge of the key characteristics linked to territory selection and distribution of this species on a landscape may inform management for this priority songbird species in the Appalachian region.

Table of Contents

List of Tables

List of Figures

Chapter 1: Introduction

The Swainson's Warbler (SWWA) is a Nearctic-Neotropical songbird that breeds across the southeastern United States. John Abbot, in 1801, was the first naturalist to paint and describe the Swainson's Warbler but John James Audubon named the bird in 1834 after receiving a specimen from John Bachman (Meanley 1971, Simpson 1984, Anich et al. 2020). The species occurs in two main geographically-disjunct regions: the Southeastern Coastal Plain and the Appalachian Mountains. The birds are generally considered absent in the Piedmont region, separating the two breeding populations.

In the coastal plains region, the SWWA is regularly found occupying stands of giant cane (*Arundinaria gigantea*), dwarf palmetto (*Sabal minor*), sweet pepperbush (*Clethra alnifolia*), and spicebush (*Lindera benzoin*); these areas often have a significant vine component, especially greenbrier (*Smilax* spp.) and grape (*Vitis* spp.; Meanley 1971, Graves 2001,2002, Benson et al. 2009, Brown et al. 2009, Graves and Tedford 2016). The Swainson's Warbler occurs in at least 2 forest types in the Appalachian Mountains: eastern hemlock (*Tsuga canadensis*) forests with rhododendron (*Rhododendron sp.*), mountain laurel (*Kalmia latifolia*), and American holly (*Ilex opaca*), and mature mountain cove hardwood forests, including yellow poplar (*Liriodendron tulipifera*), oak (*Quercus* spp.), and maple (*Acer* spp.) with understories of spicebush, greenbrier and rhododendron (Brooks and Legg 1942, Sims and DeGarmo 1948, Meanley 1971, Lanham and Miller 2006). Swainson's Warblers have also been documented elsewhere using young pine (*Pinus sp.*) plantations (Carrie 1996, Wilson and Watts 2000, Bassett-Touchell and Stouffer 2006, Graves 2015, Henry et al. 2015)

Studies done in the coastal plain have identified several habitat features related to Swainson's Warbler territory selection including dense canopy cover with disturbance gaps, dense shrub-

level vegetation, abundant leaf litter, sparse herbaceous vegetation, moist soils and substantial forest cover at the landscape scale (Meanley 1971, Eddleman 1978, Thomas et al. 1996, Graves 1998;2001;2002, Wright 2002, Bednarz et al. 2005, Benson et al. 2009, Brown et al. 2009, Anich et al. 2010, Graves and Tedford 2016, Anich et al. 2020). Aside from a nest-site selection study conducted in South Carolina (Lanham and Miller 2006), no detailed studies have examined Swainson's Warbler territory characteristics in the Appalachian portion of its range beyond basic habitat descriptions (Nicholson 1998).

The global SWWA population is estimated at 160,000 individuals (2021 estimate, Partners in Flight [PIF], Population Estimates Database, https://pif.birdconservancy.org/population-estimate-database-scores/); the 3rd lowest population estimate of all North American warbler species. Despite the relatively small population size, based on the North American Breeding Bird Survey (BBS), the SWWA breeding population increased at 2.4%/year from 1966-2022 rangewide, and increasing at 4.3%/year in Tennessee (Ziolkowski et al. 2023). PIF estimated a 67% population increase between 1970 and 2015 (Anich et al. 2020). This reported increase has led Partners in Flight to rate the SWWA as a 13 of 20 on the continental concern score scale, indicating that it is a species of relatively low conservation concern (Anich et al. 2020). Detection issues likely make status of the SWWA uncertain range-wide, with song variation, cryptic coloration/habits, and their preference for dense vegetation thickets leading to identification and detection issues. The Tennessee State Wildlife Action Plan (TN-SWAP) lists the species as "In Need of Management" due to habitat loss in west Tennessee where the bird uses bottomland hardwood forests, but little is known about the current status of the SWWA in the eastern portion of the state (Nicholson 1998).

This study is the first in depth SWWA habitat study in Tennessee and aims to address several key objectives; 1. determine which vegetation and topographic variables were most strongly related to territory selection, 2. determine if remotely-sensed metrics are as effective as, or serve as reliable proxies for ground-based metrics for predicting Swainson's Warbler territory selection, 3. determine whether resource selection in the Appalachian Mountains was consistent with resource selection in Coastal Plains population, and 4. determine the distribution of potential Swainson's Warbler habitat on the southern districts of the Cherokee National Forest, and 5. inform Swainson's Warbler monitoring and management in the southern districts of the Cherokee National forest. Chapter 2 addresses objectives 1-3 and Chapter 3 addresses objectives 4-5. Chapter 4 is a summary of the key findings of the research.

Literature Cited

Anich, N. M., T. J. Benson, and J. C. Bednarz. 2010. Factors influencing home-range size of Swainson's Warblers in eastern Arkansas. The Condor 112:149-158.

Anich, N. M., T. J. Benson, J. D. Brown, C. Roa, J. C. Bednarz, R. E. Brown, and J. G. Dickson. 2020. Swainson's Warbler (*Limnothlypis swainsonii*). Birds of the World, Cornell Lab of Ornithology, Ithaca, NY, USA.

Bassett-Touchell, C. A., and P. C. Stouffer. 2006. Habitat selection by Swainson's Warblers breeding in loblolly pine plantations in southeastern Louisiana. The Journal of Wildlife Management 70:1013-1019.

Bednarz, J. C., P. Stiller-Krehel, and B. Cannon. 2005. Distribution and habitat use of Swainson's Warblers in eastern and northern Arkansas. US Department of Agriculture, Forest Service, General Technical Report PSW-GTR-191, Jonesboro, AR.

Benson, T. J., N. M. Anich, J. D. Brown, and J. C. Bednarz. 2009. Swainson's Warbler nest-site selection in eastern Arkansas. The Condor 111:694-705.

Brooks, M., and W. C. Legg. 1942. Swainson's Warbler in Nicholas County, West Virginia. Auk 59:76-86.

Brown, J. D., T. J. Benson, and J. C. Bednarz. 2009. Vegetation characteristics of Swainson's Warbler habitat at the White River National Wildlife Refuge, Arkansas. Wetlands 29:586-597.

Carrie, N. R. 1996. Swainson's Warblers nesting in early seral pine forests in east Texas. Wilson Bulletin 108:802-804.

Eddleman, W. R. 1978. Selection and management of Swainson's Warbler habitat. M. S. thesis, University of Missouri-Columbia. 76p.

Graves, G. R. 1998. Stereotyped foraging behavior of the Swainson's Warbler (Limnothlypis swainsonii). Journal of Field Ornithology 69:121-127.

_____. 2001. Factors governing the distribution of Swainson's Warbler along a hydrological gradient in Great Dismal Swamp. Auk 118:650-664.

_____. 2002. Habitat characteristics in the core breeding range of the Swainson's Warbler. Wilson Bulletin 114:210-220.

_____. 2015. Recent large-scale colonisation of southern pine plantations by Swainson's Warbler Limnothlypis swainsonii. Bird Conservation International 25:280-293.

Graves, G. R., and B. L. Tedford. 2016. Common denominators of Swainson's Warbler breeding habitat in bottomland hardwood forest in the White River Watershed in southeastern Arkansas. Southeastern Naturalist 15:315-330.

Henry, D. R., D. A. Miller, and T. W. Sherry. 2015. Integrating wildlife conservation with commercial silviculture—demography of the Swainson's Warbler (Limnothlypis swainsonii), a migrant bird of conservation concern in southern pine forests, USA. Pages 217-235 *in,* Miodrag Zlatic. Precious Forests-Precious Earth. IntechOpen, Riejeka Croatia.

Lanham, J. D., and S. M. Miller. 2006. Monotypic nest site selection by Swainson's Warbler in the mountains of South Carolina. Southeastern Naturalist 5:289-294.

Meanley, B. 1971. Natural history of the Swainson's Warbler. North American fauna series No. 69. U.S. Department of the Interior, Washington, D.C.

Nicholson, C. P. 1998. Atlas of breeding birds of Tennessee. The University of Tennessee Press, Knoxville.

Simpson, M. B. 1984. The Artist-Naturalist John Abbot (1751-ca. 1840): Contributions to the Ornithology of the southeastern United States. The North Carolina Historical Review 61:347-390.

Sims, E., and W. DeGarmo. 1948. A study of Swainson's Warbler in West Virginia. Redstart 16:1-8.

Thomas, B. G., E. P. Wiggers, and R. L. Clawson. 1996. Habitat selection and breeding status of Swainson's Warblers in southern Missouri. The Journal of Wildlife Management 60:611-616.

Wilson, M. D., and B. Watts. 2000. Breeding bird communities in pine plantations on the coastal plain of North Carolina. Chat 64:1-14.

Wright, E. A. 2002. Breeding population density and habitat use of Swainson's Warblers in a Georgia floodplain forest. Ph. dissertation. University of Georgia,Athens.

Ziolkowski, D., M. Lutmerding, W. B. English, V. I. Aponte, and M.-A. R. Hudson. 2023. North American Breeding Bird Survey dataset 1966 - 2022: U.S. Geological Survey, https://www.usgs.gov/data/2023-release-north-american-breeding-bird-survey-dataset-1966-2022#:~:text=The%201966%2D2022%20North%20American,%2C%20and%20unidentified%20species%20groupings).

Chapter 2: Swainson's Warbler (*Limnothlypis swainsonii*) resource selection in the Appalachian Mountains on the Cherokee National Forest, Tennessee

Abstract

The Swainson's Warbler is a Nearctic-Neotropical songbird that breeds across the southeastern United States in two main, geographically-disjunct regions: the Southeastern Coastal Plains and the Appalachian Mountains. There are very few detailed habitat studies of Swainson's Warbler in the Appalachian region, and none of these studies have been conducted in Tennessee. We located and characterized the vegetation at Swainson's Warbler territories and random absence points in 2022 and 2023 on the southern ranger districts of Cherokee National Forest, Tennessee. A suite of on-the-ground vegetation and topographic covariates were assessed alongside LiDAR-derived covariates via a linear regression resource selection analysis with AIC_c model selection. Our objectives included: 1. determine which vegetation and topographic covariates were most strongly related to territory selection, 2. determine if remotely-sensed covariates were as effective as, or served as reliable proxies for ground-based covariates for predicting Swainson's Warbler territory selection, and 3. determine whether resource selection in the Appalachian Mountains was consistent with resource selection in Coastal Plains populations. Appalachian Swainson's Warblers selected territories with a comparatively dense shrubby understory, consistent with findings elsewhere in the breeding range, with percent understory cover, and visual obstruction being the top predictors of Swainson's Warbler territory selection. Remotely-sensed variables were also significant predictors of Swainson's Warbler territory selection but were weaker than the top on-the-ground covariates. LiDAR-derived vegetation covariates were not correlated with any on-the-ground vegetation covariates ($r > 0.7$). This study takes an on-the-ground and remote-sensing approach to successfully identify vegetation metrics that are related to Swainson's Warbler territory selection in the

southern Appalachian Mountains. Knowledge of the key characteristics linked to territory selection may inform management for this priority songbird species in the Appalachian region.

Introduction

The Swainson's Warbler (SWWA) is a Nearctic-Neotropical songbird that breeds across the southeastern United States within two main geographically-disjunct regions: the Southeastern Coastal Plain and the Appalachian Mountains (Meanley 1971, Anich et al. 2020). The species is generally absent from the Piedmont region, which lies between the two breeding populations. Historically, SWWA was considered a canebrake *(Arundinaria gigantea*) specialist (Brewster 1885) but has since been found in different vegetation communities range-wide. In the Coastal Plains region, the SWWA is regularly found occupying stands of giant cane, dwarf palmetto (*Sabal minor*), sweet pepperbush (*Clethra alnifolia*), or spicebush (*Lindera benzoin*), often with a significant vine component, especially greenbrier (*Smilax* spp.) and grape (*Vitis* spp.; Meanley 1971, Graves 2001, 2002, Benson et al. 2009, Brown et al. 2009, Graves and Tedford 2016). The Swainson's Warbler occurs in 2 main forest types in the Appalachian Mountains: eastern hemlock (*Tsuga canadensis*) forests with rhododendron (*Rhododendron* spp.), mountain laurel (*Kalmia latifolia*), and American holly (*Ilex opaca*) understories, and mature mountain cove hardwood forests, including yellow poplar (*Liriodendron tulipifera*), oak (*Quercus* spp.), and maple (*Acer* spp.), with understories of spicebush, rhododendron, and greenbrier (Brooks and Legg 1942, Sims and DeGarmo 1948, Meanley 1971, Nicholson 1998, Lanham and Miller 2006). Swainson's Warblers have also been documented using young pine (*Pinus sp.*) plantations in the Coastal Plain (Carrie 1996, Wilson and Watts 2000, Bassett-Touchell and Stouffer 2006, Graves 2015, Henry et al. 2015).

Studies done in the Coastal Plains have identified several habitat features related to Swainson's Warbler territory selection including dense canopy cover with disturbance gaps, dense shrub-

level vegetation, abundant leaf litter, sparse herbaceous vegetation, moist soils and substantial forest cover at the landscape scale (Meanley 1971, Eddleman 1978, Thomas et al. 1996, Graves 1998;2001;2002, Wright 2002, Bednarz et al. 2005, Benson et al. 2009, Brown et al. 2009, Anich et al. 2010, Graves and Tedford 2016, Anich et al. 2020). Very few published studies have documented SWWA habitat characteristics in the Appalachian Mountains, apart from a nest-site selection study conducted in South Carolina (Lanham and Miller 2006). No published habitat studies on Swainson's Warblers exist for Tennessee apart from general descriptions of habitat use in the Tennessee Breeding Bird Atlas (Nicholson 1998).

The global SWWA population was estimated at 160,000 individuals in 2021 (Partners in Flight, population estimates database, https://pif.birdconservancy.org/population-estimate-database-scores/), the 3rd lowest population estimate of any North American warbler species. Despite the relatively small population size, based on the North American Breeding Bird Survey (BBS), the SWWA breeding population increased at 2.4%/year from 1966-2022 range-wide, and increased at 4.3%/year in Tennessee (Ziolkowski et al. 2023). Partners in Flight (PIF) estimated a 67% population increase between 1970 and 2015 (Anich et al. 2020). Based in part on the reported population increase, the SWWA has a PIF continental concern score of 13 on a scale of 20, indicating that SWWA is a species of relatively low conservation concern (Anich et al. 2020). Detection issues likely make status of the SWWA uncertain range-wide. SWWA song variation, cryptic coloration/habits, and preference for dense vegetation thickets likely lead to identification and detection issues. The Tennessee State Wildlife Action Plan (TN-SWAP) lists the species as "In Need of Management" due to habitat loss in west Tennessee where the bird utilizes bottomland

hardwood forests, but little is known regarding the status of the SWWA in the eastern portion of the state.

Remote sensing has certain advantages over manual on-the-ground habitat measurement because of the ease and reduced cost of collecting remotely-sensed data (Nagendra et al. 2013, Corbane et al. 2015). Remote sensing is especially desirable in the case of characterizing SWWA habitat because of this species' preference for dense vegetation thickets range wide, which make traditional vegetation mensuration methods difficult and time consuming. Traditional remote-sensing sources, however, often lack vegetation structural metrics required for modeling structure-dependent species' resource selection (e.g. spectral imagery, aerial photography, national land cover database). Recent advancements in light detection and ranging (LiDAR) software, data availability and methodology have allowed researchers to derive several vegetation structural metrics from LiDAR point clouds, which have been used effectively to remotely sense habitat for other structure-dependent species (Bradbury et al. 2005, Vierling et al. 2008, Martinuzzi et al. 2009a, Martinuzzi et al. 2009b, García-Feced et al. 2011, Tattoni et al. 2012, Vierling et al. 2013, Johnston and Moskal 2017, Shanley et al. 2021, McNeil et al. 2023, Larkin et al. 2024). In this study, we employed a similar LiDAR-based methodology to collect LiDAR-derived vegetation covariates to determine if a remote-sensing approach was an effective strategy for modeling SWWA breeding habitat in the Appalachian Mountains.

This project is the first in-depth habitat study characterizing Swainson's Warbler habitat in Tennessee. Specific objectives included: 1. determine which vegetation and topographic covariates were most strongly related to territory selection, 2. determine if remotely-sensed covariates were as effective as, or were correlated with on-the-ground based covariates for

predicting Swainson's Warbler territory selection, and 3. determine whether resource selection in the Appalachian Mountains was consistent with resource selection in Coastal Plains populations.

Study Area and Methods

Study area: The study area was the Tellico and Hiwassee-Ocoee ranger districts which comprise the southern zone of the Cherokee National Forest in Monroe and Polk counties in southeastern Tennessee. This 88,000-ha region of the Cherokee National Forest represents the southernmost portion of the Blue Ridge Mountains physiographic province in Tennessee (Raitz et al. 2019). The Cherokee National Forest is primarily comprised of mature hardwood, coniferous and mixed forest types, with an interspersion of younger age class stands created via various types of timber harvest. SWWA have been previously documented in the study area during US Forest Service R8bird avian point count monitoring (Bartlett 1995).

SWWA surveys: We used a GIS road layer for the southern districts of the Cherokee National Forest to select routes along secondary roads that were >8 km in length, <1,067 m in elevation and accessible by vehicle. Minimum route length was based on survey efficiency with the goal of having at least 10 points along each route which could be surveyed on a given morning. Each selected route was preliminarily assessed to determine if portions of the route had potential Swainson's Warbler habitat (i.e., understory vegetation <3 m in height). We selected a total of 11 routes, 9 km on average, totaling 99 km (Fig. 2.1). After establishing a random starting point, we established individual survey locations on each route at 500-m intervals to eliminate

potential for double counting birds from multiple locations. Once a route was selected, we conducted 5-min point counts at each selected location twice during the breeding season each year (17 May to 30 June, 2022 and 2023). All point counts were conducted within 4 hours of sunrise on days without high winds and/or rain. Each 5-min point count included a 3-min silent listening period, a 1 min period of conspecific playback to enhance detection, and a final 1 min of silent listening (Ralph et al. 1995). When a SWWA was located at a survey point, azimuth and distance estimates were recorded from the observer to the bird. An actual location for the bird was then calculated based on the location of the observer, the azimuth and the distance. We analyzed the actual location of detected SWWA at each survey point to determine whether each recorded SWWA had been detected once or twice in a given year.

Vegetation sampling: If a SWWA was detected at a given survey point twice in a given year and its location was <150 m from the survey location, its territory was considered a candidate for vegetation mensuration. We used the lesser (closer) of the two distance estimates as the center of the plot for vegetation measurement, assuming the lesser distance was estimated with less error. From the list of candidate SWWA survey locations, 30 individuals were randomly selected for mensuration. We also randomly selected (n = 30) survey locations from roadside points where SWWA were not detected on either visit in any year for mensuration. A random azimuth (0-359 º) and distance (25 - 140 m) were generated for each randomly selected "absence" survey point to generate a random "absence" location for comparison with the "presence" points. Distance thresholds assigned to random absence locations were determined using the 10^{th} and 90^{th} percentiles of all estimated distances to birds detected during the survey period.

Acknowledging the high likelihood that the SWWA is dependent on understory structure, we applied a structure-centric approach to vegetation sampling. At each selected SWWA territory and random absence location, we measured 11 on-the-ground vegetation metrics (Table 2.1). We defined vegetation into three height categories: understory vegetation (>1 m and <3 m in height); midstory vegetation (>3 m and < the height of canopy trees) and canopy (height of dominant/co-dominant tree crowns). Percent ground cover, percent midstory cover and percent canopy cover were evaluated based on a point-intercept method at 1-m intervals along two 22.6-m transects bisecting the plot in cardinal directions (James et al. 1970). Percent ground cover types were divided into the following classifications: leaf litter (LL), bare ground (BG), course woody debris (CWD), grass (GR), forb (FO), brush (BR), water (WA), mud (MU), fern (FE), moss (MO), rock (RO), vine (VI), and cane (CA). A tube densitometer was used to determine if midstory and canopy were present above each 1-m interval on the transect. Diameter at breast height (DBH) was measured for all trees within the 11.3-m radius plot. Basal area was measured at plot center using a 2.5 m^2/ha basal area prism. Shrubs (<10 cm DBH & >1.5 m in height) were identified in a 3-m radius plot; shrub presence/ absence was analyzed binomially. Leaf litter depth was measured using a ruler at plot center and at the end of each transect (5 points per plot). We used a Nudds board to measure percent visual obstruction from plot center to the 3-m and 11.3-m intervals along the cardinal direction transects, using a 2-m tall Nudds board divided into 5 equal strata to determine percent visual obstruction (Nudds 1977). Each stratum was assigned a 1-5 ranking based on what percentage of the strata was obscured by vegetation, with 1 = 0 - 20%, 2 = 21 - 40%, 3 = 41 – 60%, 4 = 61 – 80%, 5 = 81 - 100. We examined visual

obstruction based on the average ranking of the third (middle) Nudds board strata at each territory and random absence plot because the other strata were generally correlated.

LiDAR and other remotely-sensed covariates: We accessed aerial LiDAR scanning (ALS) data for Polk (2015) and Monroe (2016) counties from the Tennessee LiDAR Program website (lidar.tn.gov). Both ALS data sets were acquired using the same scanner (Leica ALS80) with the same specifications--1064 nm wavelength, 272 kHz pulse rate, 40° scan angle, 50 Hz scan rate, and 0.2 mrad beam divergence —with the same methods-- 1981 m flight elevation at a speed of 150 knots. Resulting data have a nominal point spacing of 0.7 m, a pulse density of 2.3 pulses m^2, and comply with quality level 2 (QL2) USGS NGP base specifications v1.2. Source data were reported in Tennessee State Plane Zone NAD83(2011) US Survey Feet and were transformed to UTM (EPSG:32616) coordinates with vertical units converted to meters for processing.
ALS point cloud data were imported into and processed in R 4.3.2 (R Core Team 2023) using the lidR (Roussel et al. 2020, Roussel et al. 2024), sp (Pebesma and Bivand 2005, Bivand et al. 2008), and terra (Hijmans 2023) packages using a workflow similar to McNeil et al. (2023) and Atkins et al. (2023). First, a digital terrain model (DTM) was created using a triangular irregular network at 10 m spatial grain, then that DTM was used to normalize the point cloud for further processing. Any errant data above 60 m was filtered out. A suite of common forest and canopy structural metrics were calculated at 10 m spatial grain using the grid metrics method from the lidR package (Table 2.2) and mosaicked using terra (Hijmans 2023)

Additional landscape metrics were created at 10-m spatial grain from ALS data including mean elevation (m), the standard deviation of elevation (m), mean aspect (°), mean slope (%), and

topographic wetness index (TWI; unitless) following the workflow of Atkins et al. (In Review). Elevation and the SD of elevation approximate the influence of topography whereas aspect, slope, and TWI additionally approximate the influence of landscape position (e.g., water availability, sunlight, wind). TWI is a steady-state wetness index that quantifies the controls exerted on hydrological processes by topography and is calculated following the equation:

Eq 1. $TWI = ln\left(\frac{a}{tan\, b}\right)$

where *a* is the upslope accumulated area and *b* is the slope in radians (Beven and Kirkby 1979). Elevation metrics were derived from DTMs; additional functions and processing from the *whitebox* (Lindsay 2016, Wu and Brown 2022) package in R was used to determine aspect, slope, and TWI with mosaicking done using terra (Hijmans 2023).

We determined the distance to nearest stream using a high definition stream layer and the "near" tool in ArcGIS Pro (ESRI, Redlands, CA). Aspect was binned into eight 45° classes (North [0° to 22.5°], Northeast [22.5° to 67.5°], East [67.5° to 112.5°], Southeast [112.5° to 157.5°], South [157.5° to 202.5°], Southwest [202.5° to 247.5°], West [247.5° to 292.5°], Northwest [292.5° to 337.5°], North [337.5° to 360°].

Data Analysis

Analysis of on-the-ground and remotely-sensed metrics: We conducted a logistic regression resource selection analysis (RSA) using the on-the-ground and remotely-sensed metrics (separately), measured at territory (n = 61) and random absence (n = 62) locations. LiDAR metrics were extracted at each SWWA territory and random absence plot at a 100-m radius scale, with a 30-m grain size, similar to McNeil et al. (2023). Each variable was evaluated as a

univariate predictor of SWWA territory selection (presence/absence) in a binomial logistic regression model. All variables with $P < 0.05$ were deemed "significant" and included in further analyses (Table 2.3). To address multicollinearity, we used the vifstep function in the usdm package in R to remove all variables that had a variance inflation factor (VIF) > 3 (Naimi et al. 2014). The remaining variables were combined into a series of univariate and multivariate (additive) logistic regression models. The top model was identified via Akaike's Information Criterion for model selection, adjusted for small sample size (AIC_c), using the aictab function in the AICcmodavg package in R (Mazerolle 2023). Any models with $\Delta AIC_c < 2.0$ were considered to be worthy of further interpretation.

We also conducted a third resource selection analysis using both on-the-ground and remotely-sensed metrics to assess the effectiveness of models based on both datasets individually versus collectively.

Correlation of on-the-ground metrics with LiDAR-derived metrics: To determine if any LiDAR-derived metrics were reliable correlates for on-the-ground metrics, we calculated correlation coefficients (r) for all possible pairs of on-the-ground and remotely-sensed covariates using the cor function in R. We considered variables with a correlation coefficient $r \geq 0.70$ to be correlated with each other (Figs. 2.2, 2.3, 2.4).

Results

Roadside surveys: We recorded 112 SWWA detections (0.57 birds/km), and 120 detections (0.61 birds/km) during 2022 and 2023, respectively. Based on distance and azimuth estimates,

an estimated 80 unique individuals were located in 2022, and 90 individuals in 2023, with 125 unique territory locations identified across the two years.

RSA using on-the ground-metrics: Eleven of 28 on-the-ground covariates were related to SWWA territory selection ($P < 0.05$), including; percent canopy cover, percent midstory cover, percent understory cover, percent leaf litter cover, percent bare ground cover, visual obstruction at 3 m, visual obstruction at 11.3 m, rhododendron presence, doghobble presence, *vaccinium* spp presence, and mean DBH (Table 2.3). None of these covariates were correlated (removed via the VIF screening). The best-supported model with on-the-ground covariates contained percent understory cover ($\beta = 7.34 \pm 1.45$ SE, 95% CI [4.28, 10.40]) and visual obstruction ($\beta = 0.56 \pm 0.18$ SE, 95% CI [0.18, 0.95]), both with positive relationships with likelihood of SWWA territory selection (Figs. 2.5 & 2.6). The best-supported model explained 100% of the AIC_c weight (Table 2.4), thus no other covariates had any model weight. Mean percent understory cover was greater for territory locations ($x = 0.91 \pm 0.03$ SE) than for random absence locations ($\bar{x} = 0.55 \pm 0.03$ SE, Table 2.3). Mean visual obstruction (Nudds board- 3rd strata) was also greater for SWWA territories ($\bar{x} = 3.43 \pm 0.21$ SE) than for random absence locations ($\bar{x} = 0.88 \pm 0.16$ SE, Table 2.3).

RSA using remotely-sensed metrics: Ten of 20 remotely-sensed covariates were related to SWWA territory selection ($P < 0.05$), including; distance to water, topographic wetness index, slope, aspect, mean outer canopy height, and percent of first returns below 2 m (Table 2.3). Four additional covariates were significant (foliar height diversity, p75, p90, and p95), but were correlated and removed via the VIF screening. The best-supported model with remotely-sensed

covariates contained TWI (β = 1.50 ± 0.36, 95% CI [0.931, 2.071]) and percent of first returns below 2 m (β = -0.12 ± 0.05, 95% CI [-0.195, -0.036]; Figs. 2.7 & 2.8), with 83% of the Akaike weight (Table 2.5). There were no models with competing AIC_c values ($\Delta AIC_c < 2.0$). Mean TWI was greater for territory locations ($\bar{x}$ = 6.44 ± 0.13 SE) than for random absence locations ($\bar{x}$ = 5.11 ± 0.11 SE, Table 2.3). The percentage of first returns below 2 m was lesser for SWWA territories ($\bar{x}$ = 15.75 ± 0.64 SE) than for random absence locations ($\bar{x}$ = 18.82 ± 0.99 SE, Table 2.3).

RSA with on-the-ground and remotely-sensed metrics: Percent understory cover and visual obstruction were the leading predictors of SWWA territory selection; this, bivariate model contained 99% of the AIC_c weight (Table 2.6) There were no other competing models with LIDAR-based covariates with $\Delta AIC_c < 2.0$. Thus, these model results were identical to the RSA results containing only on-the-ground metrics.

Correlation of on-the-ground metrics with LiDAR-derived metrics: No on-the-ground metrics were correlated (> 0.60) with any of the LiDAR-derived metrics (Fig. 2.2).

Discussion

Swainson's Warbler territories in the southern districts of the Cherokee National Forest occurred on mesic sites, with a high topographic wetness index, a dense (often rhododendron) understory, and a relatively sparse canopy. Our multi-tiered resource selection analysis compared the effectiveness of on-the ground with remotely-sensed covariates as predictors of SWWA territory selection, and determined if any remotely-sensed variables served as reliable proxies for traditional on-the-ground measurements. Remotely-sensed variables were easily

obtained and can be successfully used to predict SWWA territory selection, although they were more weakly related to SWWA territory selection than several key on-the-ground understory structural covariates. The significant vegetation covariates identified in our Appalachian study included visual obstruction, percent canopy cover, percent litter cover, and percent understory cover, consistent with patterns of resource selection from Coastal Plain populations, although use of individual shrub species, such as rhododendron, differed (Brewster 1885, Carrie 1996, Graves 2001;2002, Somershoe et al. 2003, Bednarz et al. 2005, Peters et al. 2005, Bassett-Touchell and Stouffer 2006, Benson et al. 2009, Brown et al. 2009, Graves 2015, Henry et al. 2015, Graves and Tedford 2016, McNair 2019, Anich et al. 2020).

Resource selection: The best-supported on-the-ground model results confirmed that SWWA selected territories with dense understory structure in the Appalachian Mountains (Fig. 2.9). The best-supported remotely-sensed model also contained covariates that can be linked biologically with expected SWWA territory selection: TWI and percent of first returns under 2 m (Figs. 2.7 & 2.8). TWI is likely related to SWWA territory selection because moist soils help to support invertebrate abundance (Levings and Windsor 1984, Monk et al. 1985). Percent of returns below 2 m also reflects a dense understory structure; dense understory vegetation at SWWA territory plots above the 2-m level likely prevent the LiDAR pulses from reaching below 2 m, thus leading to lower values for percent returns below 2 m at territory locations. Although these two remotely-sensed covariates were significantly related to SWWA territory selection, they did not improve model performance when added into the best-supported on-the-ground model.

Many additional covariates that were not in the best-supported model were significantly related to SWWA territory selection univariately and may have biological significance as well. For example, canopy cover was lesser for territory locations (0.49 ± 0.02 SE) compared to random absence locations (0.66 ± 0.03 SE). When canopy cover is reduced to <50%, additional light to the forest floor enables additional understory development, which SWWA apparently were selecting for (Frost 1996, Bartolome and Connor 1997, Vander Yacht et al. 2017). Also, rhododendron was over three times more prevalent at territory locations (0.77 ± 0.05 SE) than at random absence locations (0.21 ± 0.05 SE). Although rhododendron was not included in the best-supported model, rhododendron cover clearly contributed to the understory cover and Nudds board metrics. The mean slope also was lesser at territory locations (14.2 ± 0.75° SE) in comparison to random absence locations (20.7 ± 0.93° SE), indicating that SWWA selected for comparatively more shallow slopes for their territories.

Habitat description and range wide comparison: Swainson's Warblers in the southern Appalachian Mountains selected mature forests with a dense shrubby understory and relatively open canopies on relatively shallow slopes with greater topographic wetness index. This description of SWWA habitat aligns well with other studies from Coastal Plains populations. In the Coastal Plains, SWWA reportedly established territories in areas with "canopy gaps", moist soil and a dense understory, often close to water (Eddleman et al. 1980, Carrie 1996, Thomas et al. 1996, Graves 2001, Somershoe et al. 2003, Peters et al. 2005, Bassett-Touchell and Stouffer 2006, Benson et al. 2009, Brown et al. 2009, Anich et al. 2010, Graves and Tedford 2016). In the Appalachians, rhododendron appeared to be important in SWWA resource selection, likely because of its dense structure and prevalence across the landscape, whereas in the Coastal

Plains, a wide array of plant species have been documented supporting SWWA territories including dwarf palmetto (*Sabal minor*), sweet pepperbush (*Clethra alnifolia*), spicebush (*Lindera benzoin*), greenbrier (*Smilax spp.*), grape (*Vitis spp.*), Chinese privet (*Ligustrum sinense*), pondberry (*L. melissifolia*), American beautyberry (Callicarpa americana), yaupon holly (Ilex vomitoria), huckleberry (*Gaylussacia spp.*), Viburnum spp., wax myrtle (*Morella cerifera*), and young pine (*pinus spp.*). Presumably these different species contribute similar structure and other resources (i.e., nest sites and invertebrates) required by SWWA.

Surprisingly, none of the LiDAR-derived understory metrics were correlated (correlation coefficient > 0.6) with any on-the-ground metrics important in SWWA resource selection. The lack of LIDAR-derived metrics correlated with on-the-ground understory metrics, which are stronger predictors of SWWA territory selection does not mean the LIDAR-derived metrics are not useful for predicting SWWA territory selection. LiDAR-derived metrics have recently been used to model other understory specialist birds species (Larkin et al 2024). However, the accuracy of the predictive models may be lower if the underlying covariate relationships are not as strong (Sakamoto et al. 1986).

Future direction and implications: This study has identified vegetation covariates that are linked with SWWA territory selection which can potentially be used to manage for SWWA in the Appalachian Mountains and will serve as a knowledge base for future habitat studies. For increased SWWA occupancy, managers may implement forest management prescriptions which either retain or support the development of dense shrubby understories under a partial canopy of mature trees (Bauhus et al. 2009).

More work is required to determine the population status and the distribution of potential habitat of SWWA in Tennessee. Populations appear to be increasing in Tennessee, based on examination of BBS data from the past 10 years (Ziolkowski et al. 2023). SWWA only occurred on a relatively limited number of locations (n = 23) on BBS routes, such that the current distribution in Tennessee is largely unknown since the breeding bird atlas was conducted from 1986-1991 (Nicholson 1998). Remote sensing with LIDAR is a promising avenue for documenting potential SWWA habitat and targeting future monitoring efforts, as it can be easily performed on a large scale (Bradbury et al. 2005, Vierling et al. 2008, García-Feced et al. 2011, Vierling et al. 2013, Zellweger et al. 2014, Johnston and Moskal 2017). A remotely-sensed modeling approach is especially attractive, for species such as the SWWA that reside in dense vegetation that is difficult to access and measure via traditional means. An important next step would be to validate the model developed in this thesis with SWWA location data from elsewhere in Tennessee to document the ability to extrapolate the model successfully to new regions in the state.

Literature Cited

Anich, N. M., T. J. Benson, and J. C. Bednarz. 2010. Factors influencing home-range size of Swainson's Warblers in eastern Arkansas. The Condor 112:149-158.

Anich, N. M., T. J. Benson, J. D. Brown, C. Roa, J. C. Bednarz, R. E. Brown, and J. G. Dickson. 2020. Swainson's Warbler (*Limnothlypis swainsonii*). Birds of the World, Cornell Lab of Ornithology, thaca, NY, USA.

Atkins, J. W., G. Bohrer , R. T. Fahey, B. S. Hardiman, T. H. Morin, A. E. Stovall, and C. M. Gough. 2018. Quantifying vegetation and canopy structural complexity from terrestrial Li DAR data using the forestr r package. Methods in Ecology and Evolution, 9(10), 2057-2066.

Atkins, J. W., J. Costanza, K. M. Dahlin, M. P. Dannenberg, A. J. Elmore, M. C. Fitzpatrick, and E. K. Tielens. 2023. Scale dependency of lidar-derived forest structural diversity. Methods in Ecology and Evolution, 14(2), 708-723.

Atkins, J.W., D.P. Aubrey, A. Horcher, R.J. McGaughey, A.E.L. Stovall, and J.L. Strunk. In Review. Estimating forest age using airborne lidar in a southeastern US forest. In revision from the Canadian Journal of Forest Research.

Bartlett, J. G.. 1995. Relative abundance of breeding birds and habitat associations of select neotropical migrant songbirds on the Cherokee National Forest, Tennessee. M.S. thesis, University of Tennessee, Knoxville.

Bartolome, W. E. F. J. W., and J. M. Connor. 1997. Understory-Canopy relationships in oak woodlands and savannas. US Department of Agriculture, Forest Service, Pacific Southwest Research Station.

Bassett-Touchell, C. A., and P. C. Stouffer. 2006. Habitat selection by Swainson's Warblers breeding in loblolly pine plantations in southeastern Louisiana. The Journal of Wildlife Management 70:1013-1019.

Bauhus, J., K. Puettmann, and C. Messier. 2009. Silviculture for old-growth attributes. Forest Ecology and Management 258:525-537.

Bednarz, J. C., P. Stiller-Krehel, and B. Cannon. 2005. Distribution and habitat use of Swainson's Warblers in eastern and northern Arkansas. US Department of Agriculture, Forest Service, General Technical Report PSW-GTR-191.

Benson, T. J., N. M. Anich, J. D. Brown, and J. C. Bednarz. 2009. Swainson's Warbler nest-site selection in eastern Arkansas. The Condor 111:694-705.

Bivand, R. S., E. J. Pebesma, V. Gómez-Rubio, and E. J. Pebesma. 2008. Applied spatial data analysis with R. Volume 747248717.Springer. New York

Bradbury, R. B., R. A. Hill, D. C. Mason, S. A. Hinsley, J. D. Wilson, H. Balzter, G. Q. Anderson, M. J. Whittingham, I. J. Davenport, and P. E. Bellamy. 2005. Modelling relationships between birds and vegetation structure using airborne LiDAR data: a review with case studies from agricultural and woodland environments. Ibis 147:443-452.

Brewster, W. 1885. Swainson's warbler. Auk 2:65-80.

Brown, J. D., T. J. Benson, and J. C. Bednarz. 2009. Vegetation characteristics of Swainson's warbler habitat at the White River National Wildlife Refuge, Arkansas. Wetlands 29:586-597.

Carrie, N. R. 1996. Swainson's Warblers nesting in early seral pine forests in East Texas. Wilson Bulletin 108:802-804.

Corbane, C., S. Lang, K. Pipkins, S. Alleaume, M. Deshayes, V. E. G. Millán, T. Strasser, J. V. Borre, S. Toon, and F. Michael. 2015. Remote sensing for mapping natural habitats and their conservation status–New opportunities and challenges. International Journal of Applied Earth Observation and Geoinformation 37:7-16.

Eddleman, W. R., K. E. Evans, and W. H. Elder. 1980. Habitat characteristics and management of Swainson's Warbler in southern Illinois. Wildlife Society Bulletin 8:228-233.

Frost, W. 1996. Understory-canopy relationships in oak woodlands and savannas/William E. Frost; James W. Bartolome; J. Michael Connor. Source: In: Pillsbury, Norman H:183-190.

García-Feced, C., D. J. Tempel, and M. Kelly. 2011. LiDAR as a tool to characterize wildlife habitat: California Spotted Owl nesting habitat as an example. Journal of Forestry 109:436-443.

Graves, G. R. 2001. Factors governing the distribution of Swainson's Warbler along a hydrological gradient in Great Dismal Swamp. Auk 118:650-664.

_____. 2002. Habitat characteristics in the core breeding range of the Swainson's Warbler. Wilson Bulletin 114:210-220.

_____. 2015. Recent large-scale colonisation of southern pine plantations by Swainson's Warbler Limnothlypis swainsonii. Bird Conservation International 25:280-293.

Graves, G. R., and B. L. Tedford. 2016. Common denominators of Swainson's Warbler breeding habitat in bottomland hardwood forest in the White River watershed in southeastern Arkansas. Southeastern Naturalist 15:315-330.

Henry, D. R., D. A. Miller, and T. W. Sherry. 2015. Integrating wildlife conservation with commercial silviculture—demography of the Swainson's Warbler (Limnothlypis swainsonii), a migrant bird of conservation concern in southern pine forests, USA. Pages 217-235 *In,* Miodrag Zlatic. Precious Forests-Precious Earth. IntechOpen, Riejeka Croatia.

Hijmans, R. 2023. terra: Spatial data analysis. R package version 1.7-39. The R Foundation for Statistical Computing.

James, F. C., J. Shugart, and H. Herman. 1970. A quantitative method of habitat description. Audubon Field Notes 24:727-736.

Johnston, A. N., and L. M. Moskal. 2017. High-resolution habitat modeling with airborne LiDAR for red tree voles. The Journal of Wildlife Management 81:58-72.

Lanham, J. D., and S. M. Miller. 2006. Monotypic nest site selection by Swainson's Warbler in the mountains of South Carolina. Southeastern Naturalist:289-294.

Larkin, J. T., C. J. Fiss, H. A. Parker, M. C. Tyree, J. Duchamp, J. L. Larkin, and D. J. McNeil. 2024. Over the river and through the woods: Multi-scale habitat associations of two at-risk bird species in riparian forests of the Central Appalachians. Forest Ecology and Management 564:121997.

Levings, S. C., and D. M. Windsor. 1984. Litter moisture content as a determinant of litter arthropod distribution and abundance during the dry season on Barro Colorado Island, Panama. Biotropica:125-131.

Lindsay, J. 2016. Whitebox GAT: A case study in geomorphometric analysis. Computers & Geosciences 95:75-84.

Martinuzzi, S., L. A. Vierling, W. A. Gould, M. J. Falkowski, J. S. Evans, A. T. Hudak, and K. T. Vierling. 2009a. Mapping snags and understory shrubs for a LiDAR-based assessment of wildlife habitat suitability. Remote Sensing of Environment 113:2533-2546.

Martinuzzi, S., L. A. Vierling, W. A. Gould, and K. T. Vierling. 2009b. Improving the characterization and mapping of wildlife habitats with lidar data: Measurement priorities for the inland Northwest, USA. Gap Analysis Bulletin 16:1-8.

Mazerolle, M. J. 2023. Version R package version 2.3.3.

McNair, D. B. 2019. Swainson's Warbler breeding distribution and habitat characteristics in bottomland hardwood forests of the Lower Piedmont in North Carolina: Importance of Chinese Privet. Southeastern Naturalist 18:510-524.

McNeil, D. J., G. Fisher, C. J. Fiss, A. J. Elmore, M. C. Fitzpatrick, J. W. Atkins, J. Cohen, and J. L. Larkin. 2023. Using aerial LiDAR to assess regional availability of potential habitat for a conservation dependent forest bird. Forest Ecology and Management 540:121002.

Meanley, B. 1971. Natural history of the Swainson's Warbler. North American fauna series No. 69. U.S. Department of the Interior, Washington, D.C.

Monk, C. D., D. T. McGinty, and F. P. Day Jr. 1985. The ecological importance of Kalmia latifolia and Rhododendron maximum in the deciduous forest of the southern Appalachians. Bulletin of the Torrey Botanical Club 122:187-193.

Nagendra, H., R. Lucas, J. P. Honrado, R. H. Jongman, C. Tarantino, M. Adamo, and P. Mairota. 2013. Remote sensing for conservation monitoring: Assessing protected areas, habitat extent, habitat condition, species diversity, and threats. Ecological Indicators 33:45-59.

Naimi, B., N. a. s. Hamm, T. A. Groen, A. K. Skidmore, and A. G. Toxopeus. 2014. Where is positional uncertainty a problem for species distribution modelling. Ecography 37:191-203.

Nicholson, C. P. 1998. Atlas of breeding birds of Tennessee. The University of Tennessee Press, Knoxville.

Nudds, T. D. 1977. Quantifying the vegetative structure of wildlife cover. Wildlife Society Bulletin 5:113-117.

Pebesma, E. and R. S. Bivand. 2005. Classes and methods for spatial data: the sp package. R News 5:9-13.

Peters, K. A., R. A. Lancia, and J. A. Gerwin. 2005. Swainson's Warbler habitat selection in a managed bottomland hardwood forest. The Journal of Wildlife Management 69:409-417.

Ralph, C. J., S. Droege, and J. R. Sauer. 1995. Managing and monitoring birds using point counts: standards and applications. Pages 161-168 In: Ralph, C. J. J. R. Sauer, and S. Droege, Sam, editors. Monitoring bird populations by point counts. General Technical Report PSW-GTR-149, US Department of Agriculture Forest Service, Pacific Southwest Research Station, Albany, CA..

Roussel, J.R., D. Auty, N. C. Coops, P. Tompalski, T. R. Goodbody, A. S. Meador, J.-F. Bourdon, F. De Boissieu, and A. Achim. 2020. lidR: An R package for analysis of Airborne Laser Scanning (ALS) data. Remote Sensing of Environment 251:112061.

Roussel, J.R., D. Auty, F. De Boissieu, A. S. Meador, and B. Jean. 2024. Package 'lidR'.

Sakamoto, Y., M. Ishiguro, and G. Kitagawa. 1986. Akaike information criterion statistics. Dordrecht, The Netherlands: D. Reidel 81:26853.

Shanley, C. S., D. R. Eacker, C. P. Reynolds, B. M. Bennetsen, and S. L. Gilbert. 2021. Using LiDAR and Random Forest to improve deer habitat models in a managed forest landscape. Forest Ecology and Management 499:119580.

Somershoe, S. G., S. P. Hudman, and C. R. Chandler. 2003. Habitat use by Swainson's warblers in a managed bottomland forest. Wilson Bulletin 115:148-154.

Tattoni, C., F. Rizzolli, and P. Pedrini. 2012. Can LiDAR data improve bird habitat suitability models? Ecological Modelling 245:103-110.

Thomas, B. G., E. P. Wiggers, and R. L. Clawson. 1996. Habitat selection and breeding status of Swainson's warblers in southern Missouri. The Journal of Wildlife Management 60:611-616.

Vierling, K. T., L. A. Vierling, W. A. Gould, S. Martinuzzi, and R. M. Clawges. 2008. Lidar: shedding new light on habitat characterization and modeling. Frontiers in Ecology and the Environment 6:90-98.

Vander Yacht, A. L., S. A. Barrioz, P. D. Keyser, C. A. Harper, D. S. Buckley, D. A. Buehler, and R. D. Applegate. 2017. Vegetation response to canopy disturbance and season of burn during oak woodland and savanna restoration in Tennessee. Forest Ecology and Management 390:187-202.

Vierling, L. A., K. T. Vierling, P. Adam, and A. T. Hudak. 2013. Using satellite and airborne LiDAR to model woodpecker habitat occupancy at the landscape scale. PloS One 8:e80988.

Wu, Q., and A. Brown. 2022. whitebox:"WhiteboxTools" R frontend. R package version 2.

Zellweger, F., F. Morsdorf, R. S. Purves, V. Braunisch, and K. Bollmann. 2014. Improved methods for measuring forest landscape structure: LiDAR complements field-based habitat assessment. Biodiversity and Conservation 23:289-307.

Ziolkowski, D., M. Lutmerding, W. B. English, V. I. Aponte, and M.-A. R. Hudson. 2023. North American Breeding Bird Survey dataset 1966 - 2022: U.S. Geological Survey, https://www.usgs.gov/data/2023-release-north-american-breeding-bird-survey-dataset-1966-2022#:~:text=The%201966%2D2022%20North%20American,%2C%20and%20unidentified%20species%20groupings).

Appendix

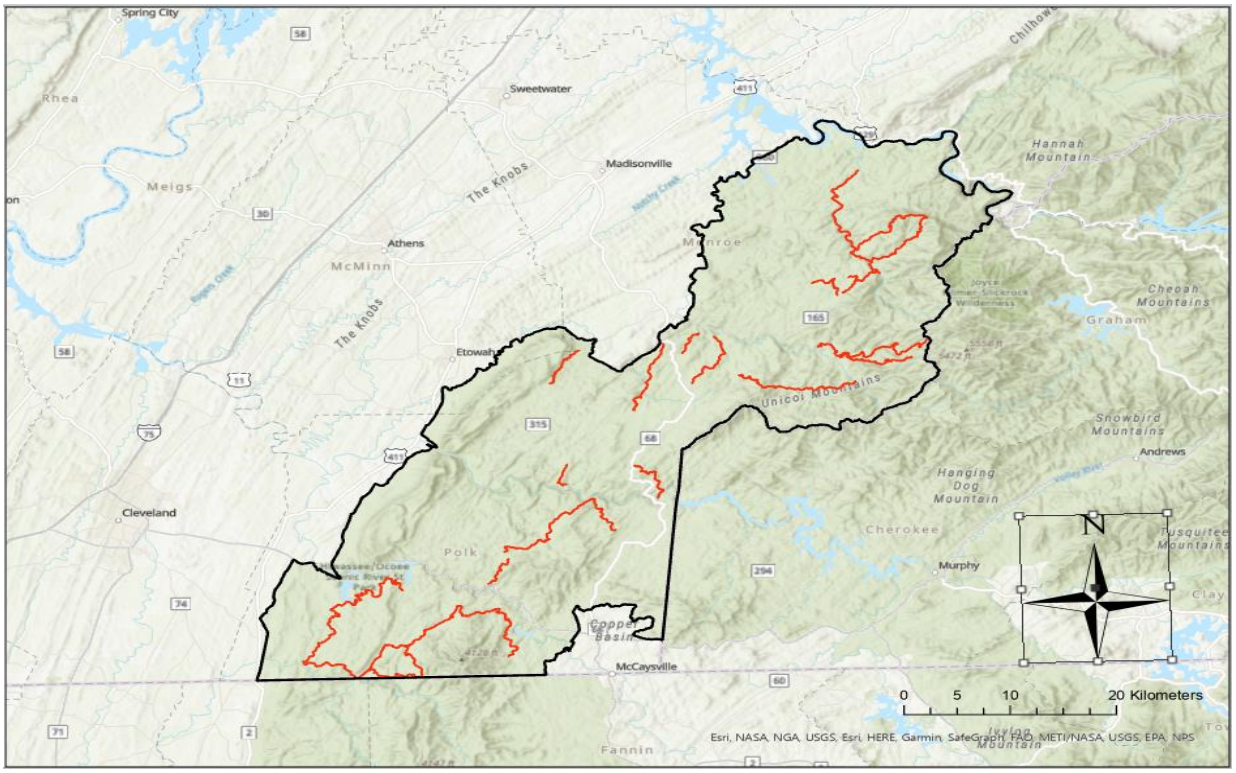

Figure 2.1. Swainson's Warblers roadside survey routes (red), Cherokee National Forest-southern ranger districts (outlined in black), Tennessee, 2022-2023.

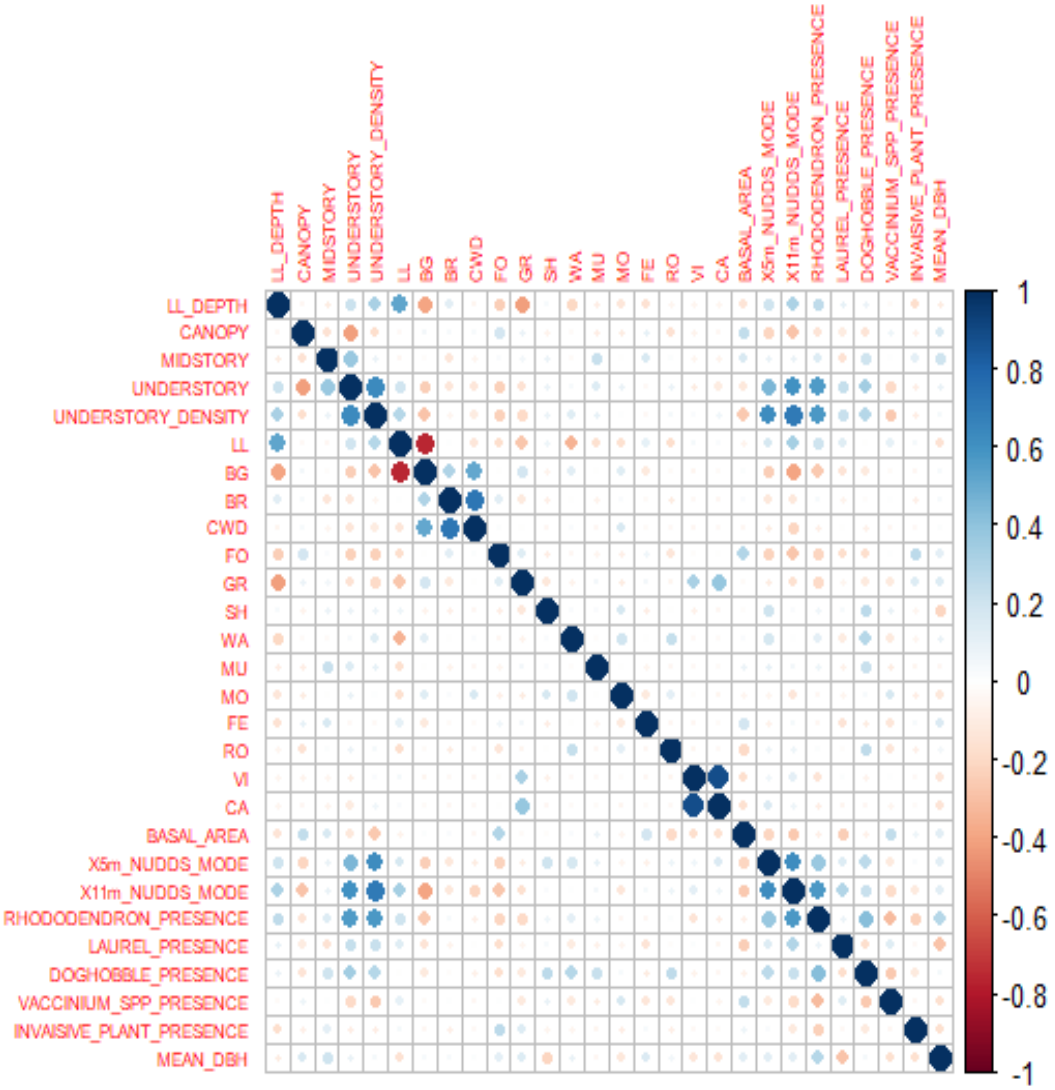

Figure 2.2. The correlation of on-the-ground metrics collected at Swainson's Warbler territories and random absence plots, southern districts of Cherokee National Forest, Tennessee, 2022-2023. Size and intensity of the symbol color indicates the strength of the correlation. Blue symbols indicate positive correlation, red symbols indicate negative correlation.

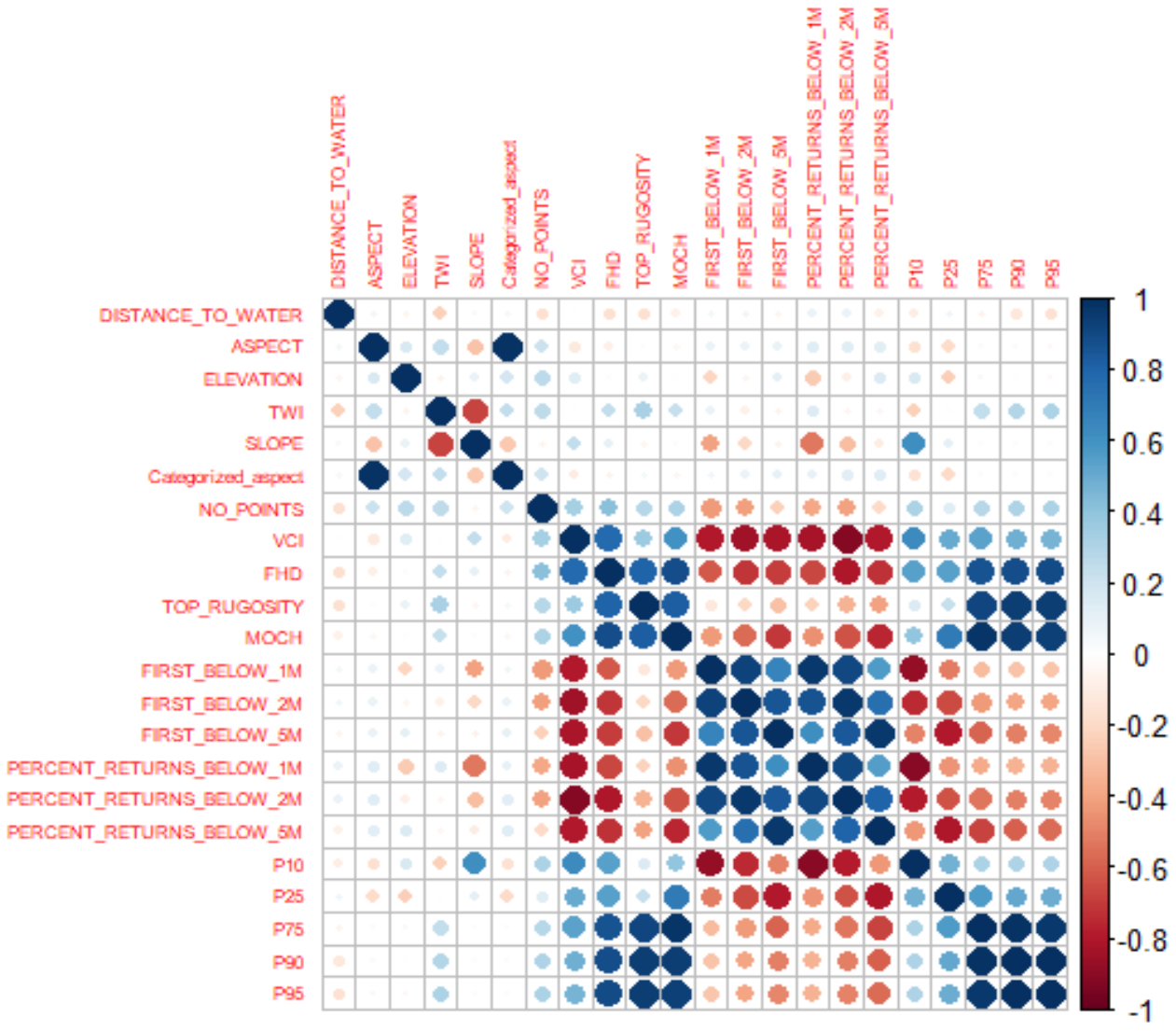

Figure 2.3. The correlation of remotely-sensed metrics collected at Swainson's Warbler territories and random absence plots, southern districts of Cherokee National Forest, Tennessee, 2022-2023. Size and intensity of the symbol color indicates the strength of the correlation. Blue symbols indicate positive correlation, red symbols indicate negative correlation.

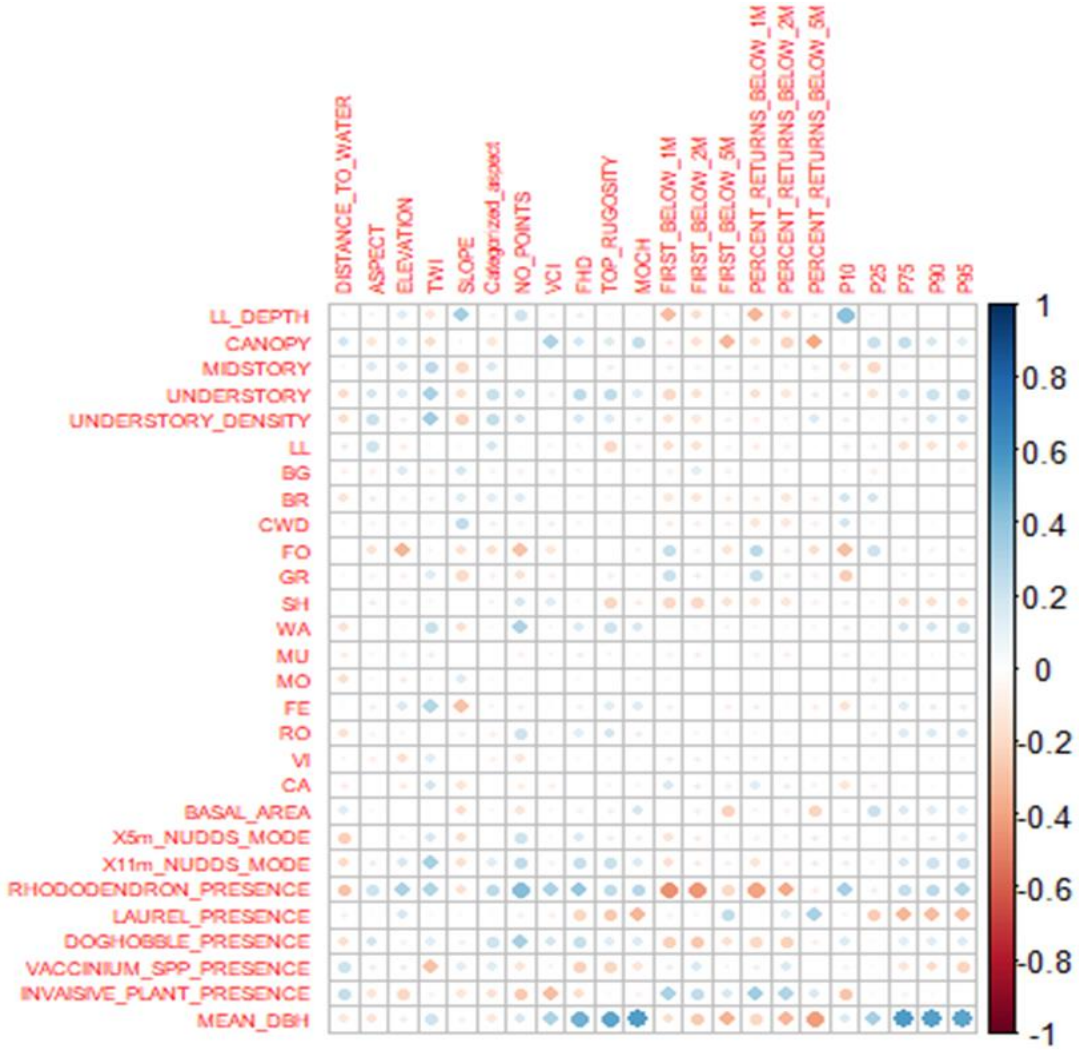

Figure 2.4. The correlation of on-the-ground and remotely-sensed metrics collected at Swainson's Warbler territories and random absence plots, southern districts of Cherokee National Forest, Tennessee, 2022-2023. Size and intensity of the symbol color indicates the strength of the correlation. Blue symbols indicate positive correlation, red symbols indicate negative correlation.

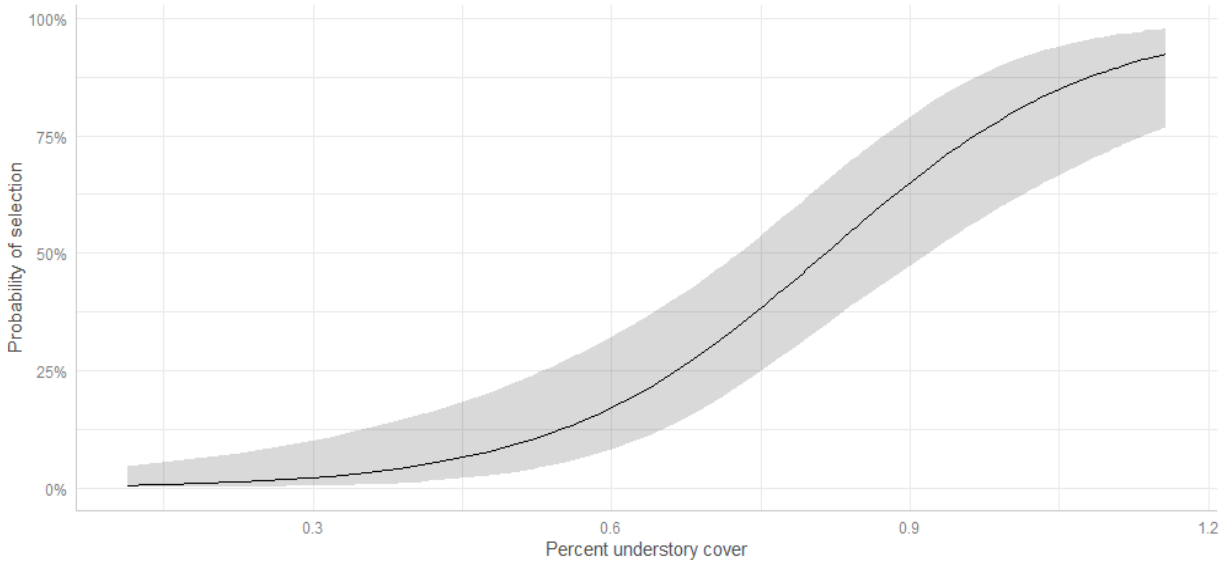

Figure 2.5. The relationship of percent understory cover and probability of Swainson's Warbler territory selection, southern districts of Cherokee National Forest, Tennessee, 2022-2023.

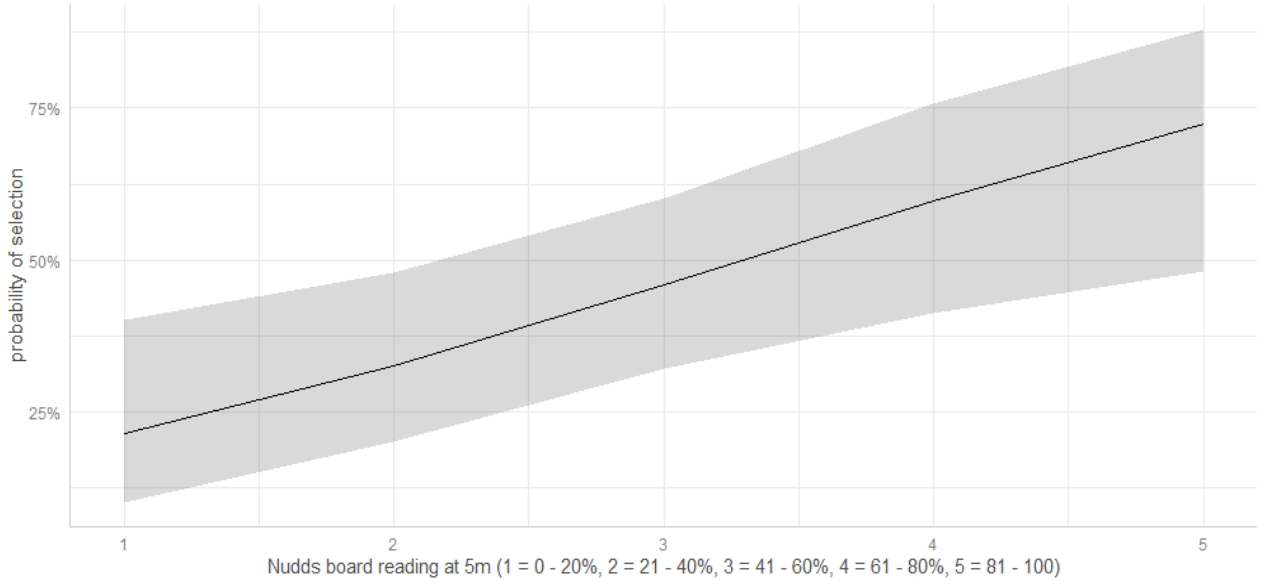

Figure 2.6. The relationship of visual obstruction (Nudds board 3rd strata) and probability of Swainson's Warbler territory selection, southern districts of Cherokee National Forest, Tennessee, 2022-2023.

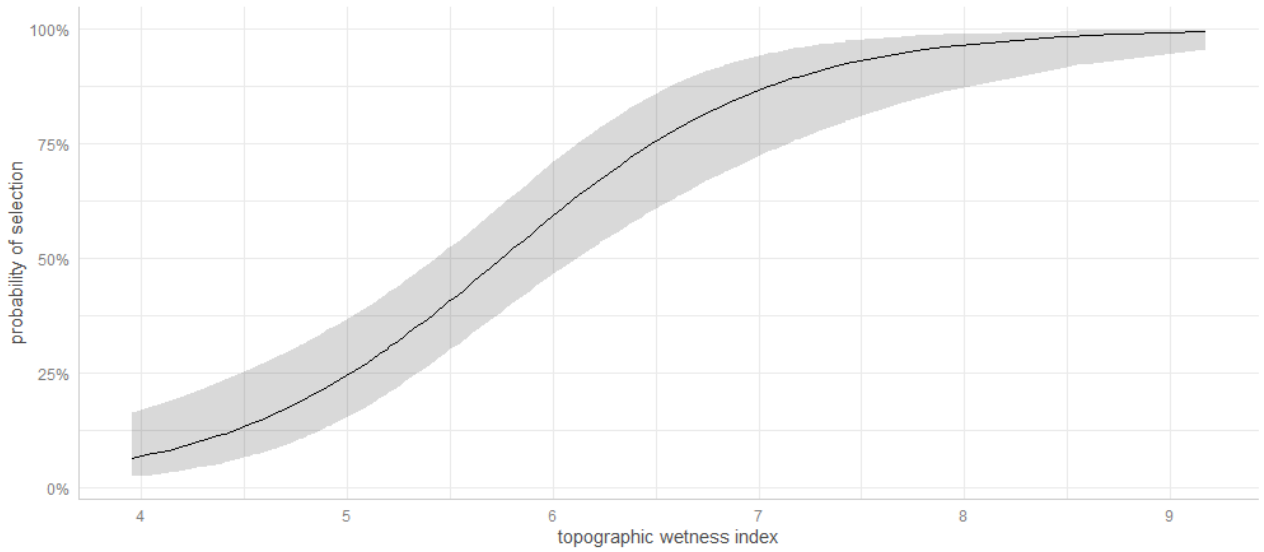

Figure 2.7. The relationship of the topographic wetness index (TWI) and probability of Swainson's Warbler territory selection, southern districts of Cherokee National Forest, Tennessee, 2022-2023.

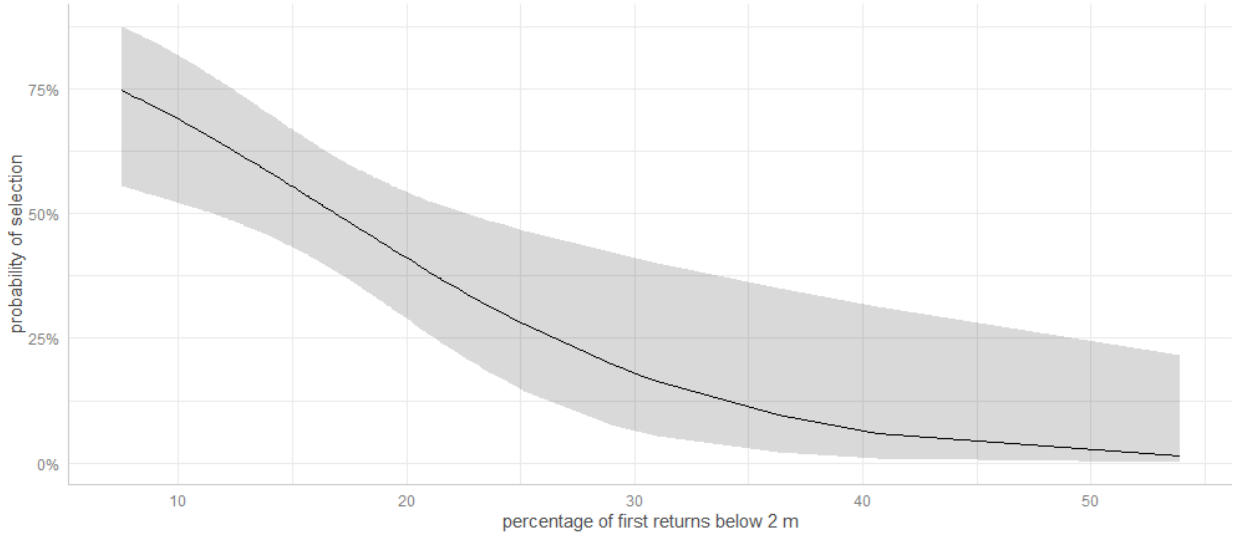

Figure 2.8. The relationship of the percentage of first returns under 2 m and probability of Swainson's Warbler territory selection, southern districts of Cherokee National Forest, Tennessee, 2022-2023.

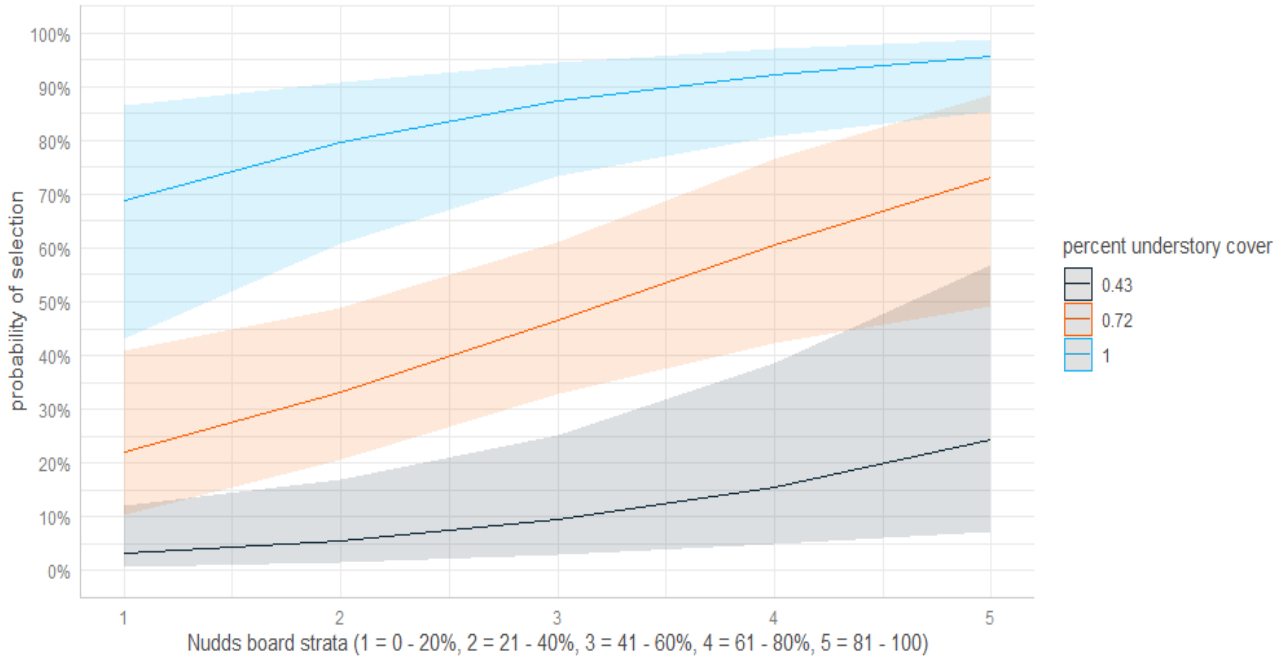

Figure 2.9. The additive effect of percent understory cover and visual obstruction on probability of Swainson's Warbler territory selection, southern districts of Cherokee National Forest, Tennessee, 2022-2023.

Table 2.1 On-the-ground Swainson's Warbler vegetation metrics names, definitions, units, variable name(s), and method of measurement, southern districts of Cherokee National Forest, Tennessee, 2022-2023.

Metric	**Definition**	**Units/ variable name**	**Measurement method**
Percent canopy cover	Percentage of plot with overstory canopy present	Percent/ CANOPY	Transect
Percent midstory cover	Percentage of plot with midstory structure present	Percent/ MIDSTORY	Transect densitometer
Percent understory cover	Percentage of plot where understory vegetation was present	Percent/ UNDERSTORY	Transect
Visual Obstruction	Percentage of visual frame covered by vegetation at a set distance	Percent/ X5m_NUDDS_MODE, X11m_NUDDS MODE	Transect Nudd's Board

Table 2.1. (cont.)

Metric	Definition	Units/ variable name	Measurement method
Basal area	Average Cross-sectional-area of tree stems within measurement plot	Meters2/ BASAL_AREA	Basal area Prism
Tree, and shrub species	Presence of shrub and tree species at habitat survey locations.	categorized by species name/ RHODODENDRON_, LAUREL_, DOGHOBBLE_, VACCINIUM_SPP_, INVAISIVE_PLANT_	Plot
Leaf litter depth	Depth of leaf litter resting on the forest floor	Centimeters/ LL_DEPTH	Transect Ruler
Percent Ground Cover	Percent composition within the plot of ground cover types	Percent/ LL, BG, BR, CWD, FOGR, SH, WA, MU, MO, FE, RO, VI, CA	Transect

Table 2.2. Remotely-sensed Swainson's Warbler vegetation variable names used for modelling, full name of each variable, units, equations used for calculation, and a description of each; southern districts of Cherokee National Forest, Tennessee, 2022-2023.

Variable	Full Name	Units	Equation	Description
MeanAngle	Mean scan angle	Degrees	$MeanAngle = \overline{\theta}$	Within grain average scan angle
MedianAngle	Median scan angle	Degrees		Within grain median scan angle
MaxAngle	Maximum scan angle	Degrees		Within grain maximum scan angle
NoPoints	Number of points	Integer count		Number of points within the grain
IQR	Interquartile range	Meters	$IQR = Q_3 - Q_1$	IQR is the range between the third (Q_3) and first quartile (Q_1)
VCI	Vertical complexity index	Unitless, 0-1	$VCI = \left(-\sum_{i=1}^{HB}[(\rho_i \ln(\rho_i))]\right) / \ln(HB)$	VCI is a complexity index calculated using the distribution of lidar returns across equally sized height bins. *HB* is the total number of height bins, and p_i is the proportional abundance of lidar returns in height bin *I* (van Ewijk et al. 2011)
Entropy		Unitless, 0-1		
FHD		Unitless		

Table 2.2 (cont.)

Variable	***Full Name***	***Units***	***Equation***	***Description***
TWI	Topographic Wetness Index	unitless	$TWI = ln\left(\frac{a}{tan\ b}\right)$	TWI is a steady-state wetness index that quantifies the controls exerted on hydrological processes by topography
VDR	Vertical distribution ratio		$VDR\ =\ (H_{Max} - H_{Median})/H_{Max}$	Vertical Distribution Ratio (Goetz et al., 2007)
Rugosity	Rugosity	Meters	$R_T = \sigma(R_{First})$	Rugosity, or top rugosity, is the standard deviation of first returns within the grain (Parker et al. 2004; Atkins et al. 2018)
MOCH	Mean outer canopy height	Meters	$MOCH\ =\ \overline{R_{First}}$	Mean outer canopy height as the mean of the first returns per pixel
Skewness	Skewness	Unitless	$Skewness = \left(3\ \times \left(\frac{Mean(z) - Median\ (z)}{\sigma(z)}\right)\right)$	A measure of the asymmetry of lidar point return distribution.
FirstBelow$_z$	First returns below z	Percentage	$Below_z = \frac{\sum R_{First} < z}{\sum R_{First}} \times 100$	Percentage of first returns below a specific height (z, meters)

Table 2-2-(cont)

$Below_z$	Returns below x	Percentage	$Below_z = \frac{\sum z < z}{\sum z} \times 100$	Percentage of all returns below a specific height (z, meters)
*p*10 … *p*95	Percentile heights	Meters	$(p_x = \text{mode}[F(x_k)])$	Height (m) at which there are X percent of returns below (i.e., p95 of 10 m indicates 95% of the returns are below this height for a given pixel.
isd	Standard deviation of intensity	Unitless		SD of lidar return intensity per pixel.
imean	Mean intensity	Unitless		Mean of lidar return intensity per pixel
DISTANCE_TO_WATER	Distance to nearest water body	Meter		Calculated in ArcGIS Pro, using the near function.
ASPECT		Categorized Aspect	Degrees	Direction of slope face. Categorized into bins established by ArcGIS pro.
SLOPE	Hill Slope	Degrees		Steepness of terrain.

Table 2.3. Mean, standard error, and p-value for each Swainson's Warbler habitat metric at territory and random absence plots; southern districts of Cherokee National Forest,

Tennessee, 2022-2023. P-values highlighted in green were deemed significant and used in resource selection analysis.

	Territories		Random Absence			
Metric	**Mean**	**SE**	**Mean**	**SE**	**P-value**	**Remotely-sensed or On-the-ground**
Leaf litter depth	2.65	0.10	2.34	0.13	0.062	On-the-ground
Percent canopy	0.49	0.02	0.66	0.03	< 0.001	On-the-ground
Percent Midstory	0.86	0.03	0.75	0.02	0.014	On-the-ground
Percent Understory	0.91	0.03	0.55	0.03	< 0.001	On-the-ground
% ground cover leaf litter	0.89	0.01	0.81	0.03	0.033	On-the-ground
% bare ground	0.02	0.01	0.09	0.02	0.020	On-the-ground
% brush ground cover	0.03	0.01	0.02	0.01	0.710	On-the-ground
% course woody debris ground cover	0.03	0.00	0.04	0.01	0.442	On-the-ground
% forb ground cover	0.02	0.01	0.06	0.02	0.059	On-the-ground
% grass ground cover	0.00	0.00	0.01	0.00	0.525	On-the-ground
% shrub ground cover	0.04	0.01	0.04	0.01	1	On-the-ground
% water cover	0.02	0.01	0.01	0.00	0.114	On-the-ground
% mud ground cover	0.01	0.00	0.00	0.00	0.371	On-the-ground
% moss ground cover	0.01	0.00	0.01	0.00	0.427	On-the-ground

Table 2.3 (cont.)

	Territories		Random Absence			
Metric	**Mean**	**SE**	**Mean**	**SE**	**P-value**	**Remotely-sensed or On-the-ground**
Basal area	102.13	4.75	105.35	6.06	0.673	On-the-ground
Mean DBH	27.67	0.85	25.04	0.79	0.029	On-the-ground
Mode of 3rd Nudds board strata at 5 m	3.43	0.21	1.88	0.16	< 0.001	On-the-ground
Mode of 3rd Nudds board strata at 11 m	4.66	0.11	3.05	0.23	< 0.001	On-the-ground
Rhododendron presence	0.77	0.05	0.21	0.05	< 0.001	On-the-ground
Laurel presence	0.21	0.05	0.21	0.05	< 0.001	On-the-ground
Doghobble presence	0.31	0.06	0.02	0.02	0.02	On-the-ground
Vaccinium spp. presence	0.13	0.04	0.34	0.06	0.008	On-the-ground
Invasive plant spp. presence	0.03	0.02	0.22	0.16	0.386	On-the-ground
Distance to nearest water	159.17	32.32	287.35	29.99	0.007	Remote
Topographic wetness index	6.44	0.13	5.11	0.11	< 0.001	Remote
Slope	14.21	0.75	20.67	0.93	< 0.001	Remote
Categorized aspect	5.50	0.17	4.65	0.17	0.001	Remote
VCI	0.92	0.00	0.92	0.00	0.318	Remote

Table 2.3 (cont.)

	Territories		Random Absence			Remote
Metric	Mean	SE	Mean	SE	P-value	Remotely-sensed or On-the-ground
MOCH	15.73	0.38	14.02	0.40	0.004	Remote
Percentage of first returns below 1 m	10.88	0.54	12.82	0.91	0.088	Remote
Percentage of first returns below 2 m	15.75	0.64	18.82	0.99	0.0175	Remote
Percentage of first returns below 5 m	25.31	0.81	27.12	1.24	0.236	Remote
Percentage of returns below 1 m	12.06	0.43	13.19	0.80	0.241	Remote
Percentage of returns below 2 m	18.20	0.49	20.19	0.82	0.058	Remote
Percentage of returns below 5 m	31.23	0.66	31.93	1.03	0.571	Remote
P10	0.94	0.04	0.91	0.04	0.675	Remote
P25	3.96	0.16	3.86	0.16	0.651	Remote
P75	20.72	0.44	18.71	0.50	0.005	Remote
P90	25.36	0.44	22.83	0.52	0.0009	Remote
P95	27.56	0.44	24.77	0.53	< 0.001	Remote
Elevation	568.71	13.10	564.14	21.40	0.854	Remote

Table 2.4. AICc, Delta AICc, AICc weight, and cumulative AICc weight of each univariate and bivariate generalized linear models in the "on-the-ground metrics only" model set for Swainson's Warblers, southern districts of Cherokee National Forest, Tennessee, 2022-2023.

Model Names	AICc	Delta AICc	AICc Wt.	Cum. Wt.
Percent Understory + 5 m visual obstruction	85.403	0.000	1.000	1.000
5 m visual obstruction + rhododendron presence	101.508	16.105	0.000	1.000
Percent canopy + 5 m visual obstruction	108.857	23.455	0.000	1.000
Percent understory + rhododendron presence	109.727	24.324	0.000	1.000
Percent understory+11m visual obstruction	110.007	24.605	0.000	1.000
5m visual obstruction + doghobble presence	111.694	26.291	0.000	1.000
5m visual obstruction + 11m visual obstruction	111.733	26.331	0.000	1.000
Percent understory + doghobble presence	112.484	27.081	0.000	1.000
percent canopy + Percent understory	113.742	28.340	0.000	1.000
Percent understory + BG	116.654	31.251	0.000	1.000
Percent understory + mean DBH	116.942	31.539	0.000	1.000
Percent understory + vaccinium presence	117.768	32.365	0.000	1.000
percent canopy + rhododendron presence	118.057	32.654	0.000	1.000
percent canopy + 11m visual obstruction	118.065	32.662	0.000	1.000
Percent understory_MOD	119.197	33.794	0.000	1.000
5m visual obstruction + vaccinium presence	119.274	33.871	0.000	1.000
mean DBH + 5m visual obstruction	119.623	34.220	0.000	1.000
Percent midstory cover + 5m visual obstruction	119.890	34.487	0.000	1.000
Percent understory + LL	120.224	34.821	0.000	1.000
Percent midstory cover + Percent understory	120.836	35.434	0.000	1.000
doghobble presence + 11m visual obstruction	122.310	36.907	0.000	1.000
BG + 5m visual obstruction	122.383	36.980	0.000	1.000
5m visual obstruction	122.847	37.444	0.000	1.000
rhododendron presence + 11m visual obstruction	123.743	38.340	0.000	1.000
LL + 5m visual obstruction	124.157	38.754	0.000	1.000
rhododendron presence + doghobble presence	128.685	43.282	0.000	1.000
Percent midstory cover + 11m visual obstruction	132.480	47.078	0.000	1.000
BG + 11m visual obstruction	132.669	47.266	0.000	1.000

Table 2.4 (cont.)

Model Names	AICc	Delta AICc	AICc Wt.	Cum. Wt.
Percent midstory cover + rhododendron presence	133.724	48.321	0.000	1.000

rhododendron presence_MODEL	134.045	48.642	0.000	1.000
LL + rhododendron presence	134.261	48.858	0.000	1.000
rhododendron presence + vaccinium presence	134.503	49.100	0.000	1.000
11m visual obstruction	134.579	49.176	0.000	1.000
mean DBH + rhododendron presence	135.363	49.961	0.000	1.000
LL + 11m visual obstruction	135.500	50.097	0.000	1.000
percent canopy + doghobble presence	136.496	51.093	0.000	1.000
percent canopy + BG	139.584	54.181	0.000	1.000
BG + doghobble presence	145.832	60.430	0.000	1.000
percent canopy + LL	145.950	60.548	0.000	1.000
percent canopy + mean DBH	146.525	61.122	0.000	1.000
percent canopy + vaccinium presence	147.322	61.919	0.000	1.000
LL + doghobble presence	147.998	62.595	0.000	1.000
mean DBH + doghobble presence	149.291	63.888	0.000	1.000
percent canopy + Percent midstory cover	151.061	65.658	0.000	1.000
doghobble presence + VACCINIUM__MOD	151.941	66.538	0.000	1.000
Percent midstory cover + doghobble presence	152.036	66.634	0.000	1.000
doghobble presence_MOD	153.083	67.680	0.000	1.000
percent canopy_MOD	153.689	68.286	0.000	1.000
BG + vaccinium presence	158.271	72.869	0.000	1.000
BG + mean DBH	159.180	73.777	0.000	1.000
Percent midstory cover + BG	160.392	74.989	0.000	1.000
LL + vaccinium presence	162.135	76.732	0.000	1.000
Percent midstory cover + vaccinium presence	162.373	76.971	0.000	1.000
BG_MOD	164.355	78.952	0.000	1.000
LL + mean DBH	164.898	79.496	0.000	1.000
Percent midstory cover + LL	165.391	79.988	0.000	1.000
LL + BG	166.325	80.922	0.000	1.000
mean DBH + vaccinium presence	166.495	81.092	0.000	1.000
Percent midstory cover + mean DBH	168.048	82.645	0.000	1.000

Table 2.4 (cont.)

Model Names	**AICc**	**Delta AICc**	**AICc Wt.**	**Cum. Wt.**
LL_MOD	170.072	84.669	0.000	1.000
mean DBH_MOD	170.826	85.423	0.000	1.000

Table 2.5. AICc, Delta AICc, AICc weight, and cumulative AICc weight of each univariate and bivariate generalized linear models in the "remotely-sensed metrics only" model set for Swainson's Warblers, southern districts of Cherokee National Forest, Tennessee, 2022-2023.

Model Names	AICc	Delta AICc	AICc Wt.	Cum. Wt.
TWI + percent of first returns below 2 m	116.544	0.000	0.831	0.831
TWI + MOCH	121.252	4.709	0.079	0.910
TWI + ASPECT	125.035	8.492	0.012	0.985
SLOPE + percent of first returns below 2 m	126.422	9.878	0.006	0.991
TWI_MOD	126.482	9.939	0.006	0.997
TWI + SLOPE	128.094	11.551	0.003	0.999
SLOPE + MOCH	132.106	15.562	0.000	1.000
ASPECT + percent of first returns below 2 m	150.080	33.536	0.000	1.000
ASPECT + SLOPE	155.846	39.303	0.000	1.000
MOCH_MOD	156.699	40.155	0.000	1.000
MOCH + percent of first returns below 2 m	157.492	40.949	0.000	1.000
ASPECT_MOD	163.629	47.085	0.000	1.000

Table 2.6. AICc, Delta AICc, AICc weight, and cumulative AICc weight of each univariate and bivariate generalized linear models in the "hybrid" model set for Swainson's Warblers, southern districts of Cherokee National Forest, Tennessee, 2022-2023.

Modnames	AICc	Delta_AICc	AICcWt	Cum.Wt
percent understory cover + 5m visual obstruction	85.403	0.000	0.994	0.994
percent understory cover + slope	95.711	10.309	0.006	1.000
5m visual obstruction + rhododendron presence	101.508	16.105	0.000	1.000
5m visual obstruction + slope	107.557	22.154	0.000	1.000
percent canopy + 5m visual obstruction	108.857	23.455	0.000	1.000
percent understory cover + rhododendron presence	109.727	24.324	0.000	1.000
percent understory cover + 11m visual obstruction	110.007	24.605	0.000	1.000
rhododendron presence + slope	111.088	25.685	0.000	1.000
5m visual obstruction + doghobble presence	111.694	26.291	0.000	1.000
5m visual obstruction + 11 m visual obstruction	111.733	26.331	0.000	1.000
percent understory cover + doghobble presence	112.484	27.081	0.000	1.000
11 m visual obstruction + slope	113.252	27.849	0.000	1.000
percent understory cover + top rugosity	113.619	28.216	0.000	1.000
percent canopy + percent understory cover	113.742	28.340	0.000	1.000
5m visual obstruction + Categorized_aspect	114.282	28.879	0.000	1.000
5m visual obstruction + top rugosity	114.593	29.190	0.000	1.000
percent understory cover + percent of returns below 2m	116.334	30.932	0.000	1.000
percent understory cover + distance to water	116.524	31.121	0.000	1.000
percent understory cover + BG	116.654	31.251	0.000	1.000
percent understory cover + mean DBH	116.942	31.539	0.000	1.000
5m visual obstruction + percent of returns below 2m	117.053	31.650	0.000	1.000
percent understory cover + vaccinium presence	117.768	32.365	0.000	1.000
percent canopy + rhododendron presence	118.057	32.654	0.000	1.000
percent canopy + 11m visual obstruction	118.065	32.662	0.000	1.000

Table 2.6 (cont.)

Modnames	AICc	Delta_AICc	AICcWt	Cum.Wt
percent understory cover + Categorized_aspect	118.368	32.966	0.000	1.000
percent understory cover_MOD	119.197	33.794	0.000	1.000
5m visual obstruction + vaccinium presence	119.274	33.871	0.000	1.000
mean DBH + 5m visual obstruction	119.623	34.220	0.000	1.000
Percent midstory cover + 5m visual obstruction	119.890	34.487	0.000	1.000
percent understory cover + LL	120.224	34.821	0.000	1.000
Percent midstory cover + percent understory cover	120.836	35.434	0.000	1.000
11 m visual obstruction + doghobble presence	122.310	36.907	0.000	1.000
BG + 5m visual obstruction	122.383	36.980	0.000	1.000
X5m_NUDDS_MOD	122.847	37.444	0.000	1.000
5m visual obstruction + distance to water	123.368	37.965	0.000	1.000
11 m visual obstruction + rhododendron presence	123.743	38.340	0.000	1.000
LL + 5m visual obstruction	124.157	38.754	0.000	1.000
11 m visual obstruction + top rugosity	124.245	38.842	0.000	1.000
percent canopy + slope	125.042	39.639	0.000	1.000
rhododendron presence_ + top rugosity	125.937	40.535	0.000	1.000
slope + percent of returns below 2m	126.422	41.019	0.000	1.000
doghobble presence_ + slope	126.889	41.486	0.000	1.000
rhododendron presence_ + doghobble presence	128.685	43.282	0.000	1.000
11 m visual obstruction + percent of returns below 2m	128.849	43.446	0.000	1.000
percent canopy + top rugosity	129.584	44.181	0.000	1.000
slope + top rugosity	130.313	44.910	0.000	1.000
11 m visual obstruction + Categorized_aspect	130.906	45.503	0.000	1.000
Percent midstory cover + 11m visual obstruction	132.480	47.078	0.000	1.000
rhododendron presence_ + percent of returns below 2m	132.483	47.080	0.000	1.000
rhododendron presence_ + Categorized_aspect	132.510	47.107	0.000	1.000
BG + 11m visual obstruction	132.669	47.266	0.000	1.000
BG + rhododendron presence	132.756	47.353	0.000	1.000
doghobble presence_ + top rugosity	132.879	47.476	0.000	1.000
11 m visual obstruction + vaccinium presence	133.377	47.974	0.000	1.000
11 m visual obstruction + distance to water	133.542	48.139	0.000	1.000

Table 2.6 (cont.)

Modnames	AICc	Delta_AICc	AICcWt	Cum.Wt
Percent midstory cover + rhododendron presence	133.724	48.321	0.000	1.000
mean DBH + 11m visual obstruction	133.861	48.458	0.000	1.000
rhododendron presence_ + distance to water	133.963	48.560	0.000	1.000
rhododendron presence_MOD	134.045	48.642	0.000	1.000
LL + rhododendron presence	134.261	48.858	0.000	1.000
rhododendron presence_ + vaccinium presence	134.503	49.100	0.000	1.000
X11m_NUDDS_MOD	134.579	49.176	0.000	1.000
mean DBH + rhododendron presence	135.363	49.961	0.000	1.000
LL + 11m visual obstruction	135.500	50.097	0.000	1.000
percent canopy + percent of returns below 2m	136.232	50.829	0.000	1.000
percent canopy + doghobble presence	136.496	51.093	0.000	1.000
percent canopy + BG	139.584	54.181	0.000	1.000
BG + slope	140.311	54.908	0.000	1.000
BG + top rugosity	140.579	55.176	0.000	1.000
doghobble presence_ + percent of returns below 2m	140.670	55.267	0.000	1.000
DIST_TO_WATER + slope	141.804	56.401	0.000	1.000
Categorized_aspect + top rugosity	143.923	58.520	0.000	1.000
vaccinium presence + slope	144.231	58.828	0.000	1.000
LL + slope	145.093	59.690	0.000	1.000
doghobble presence_ + Categorized_aspect	145.340	59.937	0.000	1.000
BG + doghobble presence	145.832	60.430	0.000	1.000
slope + Categorized_aspect	145.863	60.460	0.000	1.000
percent canopy + LL	145.950	60.548	0.000	1.000
LL + top rugosity	146.435	61.032	0.000	1.000
percent canopy + mean DBH	146.525	61.122	0.000	1.000
percent canopy + Categorized_aspect	146.608	61.205	0.000	1.000
mean DBH + slope	146.616	61.213	0.000	1.000
percent canopy + vaccinium presence	147.322	61.919	0.000	1.000
Percent midstory cover + slope	147.931	62.528	0.000	1.000
LL + doghobble presence	147.998	62.595	0.000	1.000

Table 2.6 (cont.)

Modnames	AICc	Delta_AICc	AICcWt	Cum.Wt
slope_MOD	148.449	63.047	0.000	1.000
vaccinium presence + top rugosity	149.182	63.779	0.000	1.000
mean DBH + doghobble presence	149.291	63.888	0.000	1.000
doghobble presence_ + distance to water	149.361	63.958	0.000	1.000
top rugosity + distance to water	149.931	64.528	0.000	1.000
Categorized_aspect + percent of returns below 2m	150.080	64.677	0.000	1.000
top rugosity + percent of returns below 2m	150.418	65.015	0.000	1.000
percent canopy + Percent midstory cover	151.061	65.658	0.000	1.000
Percent midstory cover + top rugosity	151.236	65.833	0.000	1.000
doghobble presence_ + vaccinium presence	151.941	66.538	0.000	1.000
Percent midstory cover + doghobble presence	152.036	66.634	0.000	1.000
percent canopy + distance to water	152.147	66.744	0.000	1.000
RUG_MOD	152.288	66.885	0.000	1.000
doghobble presence_MOD	153.083	67.680	0.000	1.000
BG + percent of returns below 2m	153.342	67.940	0.000	1.000
CAN_MOD	153.689	68.286	0.000	1.000
mean DBH + top rugosity	154.368	68.965	0.000	1.000
vaccinium presence + percent of returns below 2m	154.566	69.163	0.000	1.000
BG + Categorized_aspect	154.910	69.507	0.000	1.000
percent of returns below 2m + distance to water	155.008	69.605	0.000	1.000
vaccinium presence + Categorized_aspect	155.280	69.877	0.000	1.000
Distance to water + Categorized_aspect	155.639	70.236	0.000	1.000
Percent midstory cover + percent of returns below 2m	155.641	70.238	0.000	1.000
BG + distance to water	157.053	71.650	0.000	1.000
mean DBH + Categorized_aspect	157.935	72.532	0.000	1.000
LL + percent of returns below 2m	158.038	72.635	0.000	1.000

Table 2.6 (cont.)

Modnames	AICc	Delta_AICc	AICcWt	Cum.Wt
BG + vaccinium presence	158.271	72.869	0.000	1.000
FIRST_BELOW_2_MOD	159.100	73.697	0.000	1.000
BG + mean DBH	159.180	73.777	0.000	1.000
mean DBH + percent of returns below 2m	160.037	74.634	0.000	1.000
Percent midstory cover + BG	160.392	74.989	0.000	1.000
Percent midstory cover + Categorized_aspect	160.722	75.319	0.000	1.000
LL + Categorized_aspect	161.462	76.059	0.000	1.000
LL + vaccinium presence	162.135	76.732	0.000	1.000
Percent midstory cover + distance to water	162.359	76.956	0.000	1.000
Percent midstory cover + vaccinium presence	162.373	76.971	0.000	1.000
LL + distance to water	162.790	77.387	0.000	1.000
Aspect_MOD	163.629	78.226	0.000	1.000
vaccinium presence + distance to water	163.863	78.460	0.000	1.000
BG_MOD	164.355	78.952	0.000	1.000
LL + mean DBH	164.898	79.496	0.000	1.000
Percent midstory cover + LL	165.391	79.988	0.000	1.000
mean DBH + distance to water	166.007	80.604	0.000	1.000
LL + BG	166.325	80.922	0.000	1.000
mean DBH + vaccinium presence	166.495	81.092	0.000	1.000
Distnace to water_MOD	167.614	82.211	0.000	1.000
Percent midstory cover + mean DBH	168.048	82.645	0.000	1.000
Percent midstory cover_MOD	169.093	83.690	0.000	1.000
LL_MOD	170.072	84.669	0.000	1.000
mean DBH_MOD	170.826	85.423	0.000	1.000

Chapter 3: Modeling Swainson's Warbler (*Limnothlypis swainsonii*) relative abundance and potential habitat in the Appalachian Mountains on the Cherokee National Forest, Tennessee

Abstract

An understanding of a species' distribution and abundance and mapping potential habitat are key to developing effective conservation strategies. In this study we developed a model predicting relative abundance and potential habitat for Swainson's Warbler (*Limnothlypis swainsonii*), a Nearctic-Neotropical songbird that is a conservation priority across most of its southeastern United States breeding range. We applied our best-performing model to map potential habitat and estimate relative abundance on the 88,000-ha southern ranger districts of the Cherokee National Forest, Tennessee in the Appalachian Mountains. To develop the model, we conducted road-based point count surveys to locate Swainson's Warbler territories in 2022 and 2023. We extracted a suite of LiDAR and other remotely sensed variables at each point count location from publicly available data. Each variable was analyzed univariately and in combination with other variables using multinomial N-mixture models to determine which variables best predicted Swainson's Warbler relative abundance. The best-performing model for predicting Swainson's Warbler relative abundance included slope, mean outer canopy height, topographic wetness index, and percent of LIDAR first returns below 1 m. We detected 125 unique Swainson's Warbler territories across the two-year survey period, with an average of 1.26 territories per survey km. We estimated that 3,520 ha of potential habitat occurred on the southern ranger districts of the Cherokee National Forest. Predicted relative abundance ranged from 0.065 to 2.45 territories per point, with a mean value of 0.218. Based on our model, 55% of potential habitat was within 200 m of roads, and could be accessed for monitoring via roadside counts, whereas only 5% of potential habitat was located within less accessible wilderness areas. An estimated, 26% of potential habitat was located within 30 m of streams

and thus was regulated by current U.S. Forest Service streamside management zone guidelines. Having a better understanding of the distribution and relative abundance of this species and mapping its potential habitat on the southern ranger districts of the Cherokee National Forest will allow managers to make informed decisions when developing forest management plans for this species of conservation concern.

Introduction

Understanding the distribution and patterns of abundance for wildlife species of conservation concern is essential to developing effective conservation strategies. Predicting population size is a key objective in wildlife science, as it allows managers to assess the status of species and to determine where management is needed. Mapping relative abundance across focal management areas allows researchers and managers to examine the distribution of focal species across the landscape, predict the amount and location of potential habitat on the landscape, and evaluate the effectiveness of management actions. When managers have an in depth understanding of the distribution, relative abundance, and amount of potential habitat for a species of conservation concern, spatially-explicet, efficient management efforts can be implemented (Nichols 2014). Relative abundance mapping has previously been used to develop successful conservation initiatives in the past for the Golden-winged Warbler (*Vermivora chrysoptera*) and Northern Bobwhite (*Colinus virginianus*) among others (Twedt et al. 2007, Thogmartin 2010, Zhang et al. 2012, Bonnot et al. 2013).

Point-based counts have been used extensively to estimate avian population size and/or relative abundance. Point-based counts distributed along roadsides have been the cornerstone of long-term avian monitoring programs, such as the North American Breeding Bird Survey (Ziolkowski et al. 2023). Roadside-based counts are useful for bird monitoring due to ease of access and efficiency in terms of points monitored per unit effort (Ralph et al. 1995) and may produce unbiased estimates of abundance for some avian species that are insensitive to the presence of the road (Lituma and Buehler 2016). N-mixture models have become increasingly popular for modelling abundance based on repeated point-count data of unmarked individuals (Royle 2004, Lituma and Buehler 2016, McCaffery et al. 2016). These models are an improvement over more traditional generalized linear models because of their ability to account for imperfect detection (Royle 2004, Ficetola et al. 2018, Barão-Nóbrega et al. 2022, Goldstein and de Valpine 2022). The development of models that produce spatially-explicit predictions of potential habitat for species of conservation concern has become feasible as remote-sensing technology has improved and as statistical models have been developed to predict where on the landscape potential habitat conditions may be present (Royle 2004, Kanga 2023).

Traditional remote-sensing sources often lack vegetation structural metrics required for modeling structure-dependent species' resource selection (e.g. spectral imagery, aerial photography, national land cover database; Vierling et al. 2008). However, recent advancements in LiDAR software, data availability and methodology have allowed researchers to derive vegetation structural metrics from LiDAR point clouds, which have been used effectively to remotely sense habitat for a diversity of structure-dependent vertebrates. (Bradbury et al. 2005, Martinuzzi et al.

2009a, Martinuzzi et al. 2009b, Vierling et al. 2013, Johnston and Moskal 2017, Shanley et al. 2021, McNeil et al. 2023).

We used roadside-based, point-count data collected in 2022 and 2023, and LiDAR-derived variables extracted from 2015 and 2016 aerial LiDAR scan (ALS) to model the relative abundance and to map potential habitat of Swainson's Warblers (SWWA) on the southern ranger districts of Cherokee National Forest, Tennessee (SCNF). We chose to study the Swainson's Warbler because it is a forest understory specialist (Brewster 1885, Brooks and Legg 1942, Sims and DeGarmo 1948, Meanley 1971, Eddleman 1978, Eddleman et al. 1980, Thomas et al. 1996, Graves 2001;2002, Somershoe et al. 2003, Peters et al. 2005, Bassett-Touchell and Stouffer 2006, Benson et al. 2009, Graves and Tedford 2016, McNair 2019, Anich et al. 2020), and we wanted to determine to what extent a remote-sensing approach based on LIDAR metrics could successfully predict potential habitat. Swainson's Warbler is also a species of conservation concern across most of the southeastern United States, such that developing predictive models of relative abundance and potential habitat may be important foundations for developing conservation strategies. Remote sensing is especially desirable in the case of the SWWA because of its preference for dense vegetation thickets range wide, which make traditional vegetation mensuration methods difficult. Using LiDAR-derived metrics as predictors in multivariate n-mixture models, we modeled SWWA relative abundance across our study area to address several key objectives: 1. identify remotely-sensed metrics that are reliable predictors of Swainson's Warbler relative abundance, 2. map relative abundance for the southern districts of the Cherokee National Forest, 3. evaluate the ability of roadside surveys to monitor Swainson's Warbler populations on the study area, and 4. determine to what extent United States Forest Service (USFS) streamside management zones

(SMZs) can be used to regulate management of potential Swainson's Warbler habitat. With only one published study on SWWA habitat use in the Appalachian Mountains portion of its breeding range (Lanham and Miller 2006) other than general descriptions of SWWA habitat (Nicholson 1998), this study will additionally help fill in that key knowledge gap for this species of conservation concern.

Study Area and Methods

Study area: The study area included the Tellico and Hiwassee-Ocoee Ranger Districts in the south zone of the Cherokee National Forest in Monroe and Polk counties in southeastern Tennessee. This 88,000-ha region of the Cherokee National Forest represents the southernmost portion of the Blue Ridge Mountains physiographic province in Tennessee. The Cherokee National Forest is primarily comprised of mature hardwood, coniferous and mixed forests, with an interspersion of younger age class stands created by timber harvest. SWWA have been previously infrequently documented in the study area during the USFS Region 8 avian point count monitoring (Bartlett 1995).

SWWA surveys: We used a GIS road layer for the southern districts of the Cherokee National Forest to select routes along secondary roads that were >8 km in length, <1, 067 m in elevation and accessible by vehicle. Minimum route length was based on survey efficiency, with the goal of having at least 10 points along each route which could be surveyed on a given morning. Each selected route was preliminarily assessed to determine if the route had potential Swainson's Warbler habitat (i.e., understory vegetation <3 m in height) along a portion of the route. A total of 11 routes were selected, ~10 km on average, and totaling 99 km (Fig. 3.1). After establishing a

random starting point, we established individual survey locations at 500-m intervals to eliminate potential for double counting birds from multiple locations. Once a route was selected, we conducted 5-min point counts at each selected location twice during the breeding season each year (17 May to 30 June, 2022 and 2023). All point counts were conducted within 4 hours of sunrise on days without high winds and/or rain. Each 5-min point count included a 3-min silent listening period, followed by 1 min of conspecific playback to enhance a 1-min period of conspecific playback to enhance detection, and a final 1-min silent period (Ralph et al. 1995). Detection covariates including date, time, and distance to water (noise) were modeled as observation covariates (p) in n-mixture models. We compared the Akaike's Information Criterion (AIC_c) score of each of the n-mixture models with observational covariates to a null model via the aictab function in the AICcmodavg package in R to determine if observational covariates had an effect on detection probability (Mazerolle 2023).

LiDAR measurements: We extracted 29 LiDAR variables within a 100-m radius of all point count locations (Table 3.1). We accessed ALS scanning data for Polk (2015) and Monroe (2016) counties from the Tennessee LiDAR Program website (https://experience.arcgis.com/experience/299f1588ebe74039ab9227b265c49849/page/Current-LIDAR-Data/). Both ALS data sets were acquired using the same scanner (Leica ALS80) with the same specifications --1064 nm wavelength, 272 kHz pulse rate, 40° scan angle, 50 Hz scan rate, and 0.2 mrad beam divergence —with the same methods-- 1981 m flight elevation at a speed of 150 knots. Although the ALS data were collected from 2015 and 2016, and SWWA data were collected from 2022 and 2023, we assume that the LIDAR data were representative of forest conditions during the SWWA survey period because <1% of the forest area (< 880 ha) on

the southern districts had been disturbed via timber harvest or canopy-removal natural disturbances (e.g., windstorm blowdowns) during the intervening period (Cherokee National Forest, unpublished data). Resulting data have a nominal point spacing of 0.7 m, a pulse density of 2.3 pulses m^2, and comply with quality level 2 (QL2) USGS NGP base specifications v1.2. Source data were reported in Tennessee State Plane Zone NAD83 (2011) US Survey Feet and were transformed to UTM (EPSG:32616) coordinates with vertical units converted to meters for processing.

ALS point cloud data were imported into and processed in R 4.3.2 (R Core Team 2023) using the lidR (Roussel et al. 2020, Roussel et al. 2024), sp (Pebesma and Bivand 2005, Bivand et al. 2008), and terra (Hijmans 2023) packages using a workflow similar to McNeil et al. (2023) and Atkins et al. (2023). First, a digital terrain model (DTM) was created using a triangular irregular network at 10-m spatial grain, then that DTM was used to normalize the point cloud for further processing. Any errant data above 60 m was filtered out. A shapefile of the southern districts of the Cherokee National forest was used to crop the LiDAR raster to only display the national forest using the mask function in the raster package (Hijmans et al. 2013). A suite of common forest and canopy structural metrics were calculated at 10-m spatial grain using the grid metrics method from the lidR package (Table 3.1) and mosaicked using terra (Hijmans 2023).

Additional landscape metrics were created at 10-m spatial grain from ALS data including mean elevation (m), the standard deviation of elevation (m), mean aspect (°), mean slope (%), and topographic wetness index (TWI; unitless) following the workflow of Atkins et al. (In Review). Elevation and the SD of elevation approximate the influence of topography whereas aspect,

slope, and TWI approximate the influence of landscape position (e.g., water availability, sunlight, wind). TWI is a steady-state wetness index that quantifies the controls exerted on hydrological processes by topography and is calculated following the equation:

Eq 1. $TWI = ln\left(\frac{a}{tan\, b}\right)$

where *a* is the upslope accumulated area and *b* is the slope in radians (Beven and Kirkby 1979). Elevation metrics were derived from DTMs and additional functions and processing from the *whitebox* (Lindsay 2016, Wu and Brown 2022) package in R were used to determine aspect, slope, and TWI, with mosaicking done using terra (Hijmans 2023).

Modeling relative abundance: We predicted SWWA relative abundance (territories per point location) using N-mixture models of LiDAR-derived vegetation and topographic metrics (Table 3.1). LiDAR metrics were extracted and averaged at each SWWA point-count location at a 100-m radius scale, with a 30-m grain size, similar to McNeil et al. (2023). Each raster was clipped to the boundary of the SCNF using the mask function in raster package in R. (Hijmans et al. 2013).

We evaluated each covariate as a univariate predictor of SWWA relative abundance in a multinomial N-mixture model. All variables with $P < 0.05$ were deemed "significant" and were included in further analyses. To address multicollinearity, we used the vifstep function in the usdm package to remove variables that had a variance inflation factor (VIF) > 3 (Naimi et al. 2014). All remaining univariately significant, uncorrelated variables were combined into a "full" N-mixture model for evaluation. We assessed the full model via bootstrap analysis with three fit statistics (sum-of-squared errors, Chi-squared, and Freeman-Tukey) to determine goodness of fit, using the parboot function from the unmarked package in R (Fiske and Chandler 2011). We

removed one variable from the full model set and re-ran the model fit and performance tests iteratively to determine whether a reduced model set improved fit and performance. Using this approach, we identified the best-performing model for use in predicting relative abundance.

Based on the best-performing model, we predicted relative abundance across the LiDAR raster using the exp function in R (Fig. 3.2). We used the clip function in ArcGIS Pro to remove all locations > 1,067 m in elevation because SWWA distribution is generally restricted to below this threshold. We overlayed roads and streams onto the predictive map in ArcGIS Pro. We arbitrarily considered map pixels with a relative abundance > 0.49 to be potential habitat. We used the con tool in ArcGIS Pro to assign all potential SWWA habitat pixels a value of 1; all other pixels were assigned a value of 0 and used the crop tool to count the number of pixels by value within 200 m of a road, 30.5 m of a stream, and in wilderness areas. Distance thresholds were determined based on the United States Forest Service streamside management zone guidelines and the maximum detection distance recorded during our point count surveys (Williams et al. 2004). The number of pixels previously determined as potential habitat was multiplied by the area of our pixel size (30 m X 30 m) and converted to hectares.

Results

Roadside survey results: We recorded 112 SWWA detections along 196 km of survey route (0.57 birds/km), and 120 detections along 196 km of survey route (0.61 birds/km) during 2022 and 2023, respectively. In 2022, SWWA were detected at 70 (35.3%) survey locations and were absent at 128 (64.7%) locations. In 2023 SWWA were detected at 65 (32.8%) locations and absent at 133 (67.2%) locations. We analyzed the point-count data at each survey point to

determine whether each recorded SWWA had been detected once or twice in a given year; an estimated 80 unique individuals were located in 2022, and 90 individuals in 2023. Based on limited color-banding and resighting data (n = 30) from 2021 and 2022, we assumed that if a territory was occupied in two consecutive seasons, it was occupied by the same individual. Based on this assumption, we estimated that we detected a minimum of 120 unique individual male Swainsons' Warblers (~50 birds returned in 2023) over the course of our two-year survey period. Date, time, and distance to water (noise), were evaluated as observation covariates (p) in N-mixture models and were found to have no significant effect on detection. All N-mixture models containing observational covariates had greater AIC_c scores than the null model, so no detection covariates were included in the N-mixture modelling. The detection probability was 0.471 ± 0.08 SE and 0.411 ± 0.09 SE, in 2022 and 2023, respectively.

N-mixture modelling: The best-performing model fit the data reasonably well based on three goodness of fit tests: error sums-of-squares (P = 0.574), Chi-squared (P = 0.914), and Freeman-Tukey (P = 0.435). The best-performing model contained 4 predictors; TWI, slope, MOCH, and percent of first returns below 1 m. Predicted relative abundance ranged from 0.065 to 2.45 birds/point, with a mean value of 0.22. Topographic wetness index (β = 0.677 ± 0.179) displayed a positive relationship to SWWA relative abundance, whereas slope (β = -0.049 ± 0.022), MOCH (β = -0.009 ± 0.043), and percent of first returns below 1 m (β = -0.129 ± 0.032) were negatively related.

Potential Habitat: Based on the model, we predicted there were 3,520 ha of potential SWWA habitat on the Ocoee and Tellico ranger districts of the Cherokee National Forest in 2022-2023.

An estimated 1,918 ha (55%) of the total potential SWWA habitat were within 200 m of an established road. An additional 191 ha (5%) were located within wilderness areas. A total of 916 ha (26%) of potential SWWA habitat were located within streamside management zones.

Discussion

We identified a suite of four remotely-sensed covariates which were significant predictors of SWWA relative abundance. We used these covariates to map relative abundance and potential habitat for a forest understory specialist, the Swainson's Warbler, a species of conservation concern breeding in the southeastern United States. We determined that the southern districts of the Cherokee National Forest had ~3,500 ha of potential SWWA habitat, much of which is accessible via road, and has potential to be incorporated into current SMZ guidelines. Having spatially-explicit abundance and potential habitat maps can be used to develop conservation strategies for species of conservation concern, such as the Swainson's Warbler. The Cherokee National Forest, for example, based on these models, has the opportunity to include Swainson's Warbler in their periodic forest management planning process.

Our best performing model contained four variables, each of which can be biologically linked to SWWA resource selection. Lower average MOCH can be related to the presence of canopy gaps, which SWWA are known to use (Meanley 1971, Graves 2001;2002, Bassett-Touchell and Stouffer 2006, Brown et al. 2009, Graves and Tedford 2016, McNair 2019, Anich et al. 2020). The β coefficient confidence interval for MOCH overlapped zero, however, implying that this covariate was not a strong predictor of relative abundance. MOCH was retained in the model because it improved model fit and performance. A positive correlation with TWI could be caused by the tendency for SWWA to select for dense rhododendron (*Rhododendron maximum*), which

prefers wetter sites (Monk et al. 1985). Rhododendron presence is also likely related to another variable that appeared in the top model; percent of returns below 1 m. A dense rhododendron understory likely prevents LiDAR first returns from reaching the 1 m height threshold as the rhododendron layer intercepts the laser pulse. The relationship, then, is likely responsible for the negative correlation with percent of returns below 1 m. Less steep slopes also were positively correlated with SWWA abundance, apparently linked to increased wetness and leaf accumulation compared to steeper slopes. Greater soil moisture and leaf litter depth both may contribute to more abundant arthropod communities, and increased foraging potential (Levings and Windsor 1984, Graves 1998).

Our relative abundance model was useful for addressing two specific management-related questions for the Cherokee National Forest: 1. To what extent are roadside counts adequate for monitoring SWWA populations and 2. How much potential SWWA habitat are covered by SMZ management guidelines.

The road coverage of the study area was extensive, providing access to many of the areas where we predicted SWWA to occur, but road coverage was sparse in the northeast and southern portions of the forest because of the designation of Citico Creek, Bald River, Little Frog and Big Frog wilderness areas (Fig. 3.3). Wilderness areas are not accessible by road but are accessible on foot with limited trail access. Based on this assessment, a roadside-based monitoring strategy using 5-min point counts with playback generated reasonable detection probabilities (i.e., >40%) and appeared to be adequate for monitoring the relative abundance of this species

although we did not specifically evaluate the potential for roadside bias (positive or negative) related to SWWA occurrence

United States Forest Service guidelines require buffers around permanent (30.5 m) and intermittent (15.25 m) streams on the national forest (Williams et al. 2004). These buffers are established to address a variety of objectives including water quality, erosion control, woody debris recruitment, and biodiversity management, and are managed in a variety of ways (Revised Land and Resource Management Plan, Cherokee National Forest, 2004, https://www.fs.usda.gov/Internet/FSE_DOCUMENTS/stelprdb5269436.pdf). For the Cherokee National Forest, no timber harvest is generally conducted within the SMZs unless there is a specific need in terms of endangered species management or management of invasive species. In the Appalachian Mountains, SWWA occur under mature forest canopies with canopy gaps created by natural tree mortality, which allows for light to reach the understory and facilitate understory (shrub) development (Bauhus et al. 2009). Streams likely provide similar canopy gap structure by restricting tree growth within the stream boundaries. Based on our estimates, 26% of potential SWWA habitat was located within 30 m of streams and is therefore being managed under current SMZ guidelines. Although SMZ guidelines were not created specifically for SWWA habitat protection, SMZ guidelines do effectively protect SWWA habitat on the Cherokee National Forest.

Future directions and management implications: The relative abundance model has been useful in addressing two specific management questions but there are additional opportunities to address important forest management questions with the model. For example, to date there

have been very few studies which have evaluated the effects of timber harvest on SWWA resource selection, relative abundance, and potential habitat. The model could be applied to evaluate the effects of various harvest prescriptions on predicted SWWA relative abundance and potential habitat, preferably in a before-after control- impact (BACI) experimental design (Smith 2002). Additionally, the wilderness areas on the southern districts of the Cherokee National Forest have been largely un-surveyed for breeding birds. The extensive trail system in these areas offers an opportunity to determine the status of SWWA populations in these areas, without the potential for roadside bias. The model could be used to map potential habitat in wilderness areas overlaid with the trail system, so that an effective monitoring strategy could be developed in areas where the species is likely to occur (Fig. 5).

Finally, the Cherokee NF makes extensive use of prescribed burning to reduce fuel loads, to enhance wildlife habitat, and to enhance oak regeneration (Revised Land and Resource Management Plan, Cherokee National Forest, 2004, https://www.fs.usda.gov/Internet/FSE_DOCUMENTS/stelprdb5269436.pdf). Published studies from elsewhere (e.g., Everitts et al. 2015) suggest that prescribed burning may increase territory size and reduce habitat quality for SWWA to the extent that prescribed burning removes understory cover. Given this potential adverse effect, it would be important to overlay predicted SWWA relative abundance with prescribed fire maps to understand the potential for this effect on the Cherokee National Forest.

Swainson's Warblers were identified in the Tennessee State Wildlife Action Plan (TN-SWAP) as 'In Need of Management', but little is known about their current statewide distribution. The

North American Breeding Bird Surveys is inadequate because only ~ 30 routes are currently surveyed annually with relatively few detections of SWWA. The Tennessee Breeding Bird Atlas mapped statewide SWWA distribution but fieldwork was conducted >30 years ago (Nicholson 1998) and may not representative of the current distribution given the recent population increases. For that reason, an up-dated distribution map for Tennessee would be useful as a foundation for developing a conservation strategy for this species. Validation of the model with occurrence data (possibly E-bird records) statewide and then application of the model would be important next steps in developing conservation strategies for Swainson's Warblers in Tennessee.

Literature Cited

Anich, N. M., T. J. Benson, J. D. Brown, C. Roa, J. C. Bednarz, R. E. Brown, and J. G. Dickson. 2020. Swainson's Warbler (*Limnothlypis swainsonii*). Birds of the World, Cornell Lab of Ornithology, Ithaca, NY, USA.

Atkins, J. W., G. Bohrer , R. T. Fahey, B. S. Hardiman, T. H. Morin, A. E. Stovall, and C. M. Gough. 2018. Quantifying vegetation and canopy structural complexity from terrestrial Li DAR data using the forestr r package. Methods in Ecology and Evolution, 9(10), 2057-2066.

Atkins, J. W., J. Costanza, K. M. Dahlin, M. P. Dannenberg, A. J. Elmore, M. C. Fitzpatrick, and E. K. Tielens. 2023. Scale dependency of lidar-derived forest structural diversity. Methods in Ecology and Evolution, 14(2): 708-723.

Atkins, J.W., D.P. Aubrey, A. Horcher, R.J. McGaughey, A.E.L. Stovall, and J.L. Strunk. In Review. Estimating forest age using airborne lidar in a southeastern US forest. In revision from the Canadian Journal of Forest Research.

Barão-Nóbrega, J. A. L., M. González-Jaurégui, and R. Jehle. 2022. N-mixture models provide informative crocodile (Crocodylus moreletii) abundance estimates in dynamic environments. PeerJ 10:e12906.

Bartlett J.G. 1995. Relative abundance of breeding birds and habitat associations of select neotropical migrant songbirds on the Cherokee National Forest, Tennessee. M.S. thesis, University of Tennessee, Knoxville.

Bassett-Touchell, C. A., and P. C. Stouffer. 2006. Habitat selection by Swainson's Warblers breeding in loblolly pine plantations in southeastern Louisiana. The Journal of Wildlife Management 70:1013-1019.

Bauhus, J., K. Puettmann, and C. Messier. 2009. Silviculture for old-growth attributes. Forest Ecology and Management 258:525-537.

Benson, T. J., N. M. Anich, J. D. Brown, and J. C. Bednarz. 2009. Swainson's Warbler nest-site selection in eastern Arkansas. The Condor 111:694-705.

Bivand, R. S., E. J. Pebesma, V. Gómez-Rubio, and E. J. Pebesma. 2008. Applied spatial data analysis with R. Volume 747248717.Springer. New York

Bonnot, T. W., F. R. Thompson III, J. J. Millspaugh, and D. T. Jones-Farrand. 2013. Landscape-based population viability models demonstrate importance of strategic conservation planning for birds. Biological Conservation 165:104-114.

Bradbury, R. B., R. A. Hill, D. C. Mason, S. A. Hinsley, J. D. Wilson, H. Balzter, G. Q. Anderson, M. J. Whittingham, I. J. Davenport, and P. E. Bellamy. 2005. Modelling relationships between birds and vegetation structure using airborne LiDAR data: a review with case studies from agricultural and woodland environments. Ibis 147:443-452.

Brewster, W. 1885. Swainson's warbler. The Auk 2:65-80.

Brooks, M., and W. C. Legg. 1942. Swainson's Warbler in Nicholas County, West Virginia. The Auk 59:76-86.

Brown, J. D., T. J. Benson, and J. C. Bednarz. 2009. Vegetation characteristics of Swainson's warbler habitat at the White River National Wildlife Refuge, Arkansas. Wetlands 29:586-597.

Eddleman, W. R. 1978. Selection and management of Swainson's Warbler habitat. Master's thesis, University of Missouri--Columbia.

Eddleman, W. R., K. E. Evans, and W. H. Elder. 1980. Habitat characteristics and management of Swainson's Warbler in southern Illinois. Wildlife Society Bulletin 8:228-233.

Everitts, J. L., Benson, T. J., Bednarz, J. C., and Anich, N. M. (2015). Effects of prescribed burning on swainson's warbler home-range size and habitat use. *Wildlife Society Bulletin*, *39*(2), 292-300.

Ficetola, G. F., B. Barzaghi, A. Melotto, M. Muraro, E. Lunghi, C. Canedoli, E. Lo Parrino, V. Nanni, I. Silva-Rocha, and A. Urso. 2018. N-mixture models reliably estimate the abundance of small vertebrates. Scientific Reports 8:10357.

Fiske, I., and R. Chandler. 2011. Unmarked: an R package for fitting hierarchical models of wildlife occurrence and abundance. Journal of Statistical Software 43:1-23.

Goldstein, B. R., and P. de Valpine. 2022. Comparing N-mixture models and GLMMs for relative abundance estimation in a citizen science dataset. Scientific Reports 12:12276.

Graves, G. R. 1998. Stereotyped foraging behavior of the Swainson's Warbler. Journal of Field Ornithology 69:121-127.

_____. 2001. Factors governing the distribution of Swainson's Warbler along a hydrological gradient in Great Dismal Swamp. The Auk 118:650-664.

_____. 2002. Habitat characteristics in the core breeding range of the Swainson's Warbler. The Wilson Bulletin 114:210-220.

Graves, G. R., and B. L. Tedford. 2016. Common denominators of Swainson's Warbler breeding habitat in bottomland hardwood forest in the White River Watershed in southeastern Arkansas. Southeastern Naturalist 15:315-330.

Hijmans, R. 2023. terra: Spatial Data Analysis. R package version 1.7-39. The R Foundation for Statistical Computing.

Hijmans, R. J., J. Van Etten, M. Mattiuzzi, M. Sumner, J. Greenberg, O. Lamigueiro, A. Bevan, E. Racine, and A. Shortridge. 2013. Raster package in R. Version. Https://Mirro Rs. Sjtug. Sjtu. Edu. Cn/Cran/Web/Packa Ges/Rast er/Raster. Pdf.

Johnston, A. N., and L. M. Moskal. 2017. High-resolution habitat modeling with airborne LiDAR for red tree voles. The Journal of Wildlife Management 81:58-72.

Kanga, S. 2023. Advancements in remote sensing tools for forestry analysis. Sustainable Forestry 6:1-24.

Lanham, J. D., and S. M. Miller. 2006. Monotypic nest site selection by Swainson's Warbler in the mountains of South Carolina. Southeastern Naturalist 5:289-294.

Levings, S. C., and D. M. Windsor. 1984. Litter moisture content as a determinant of litter arthropod distribution and abundance during the dry season on Barro Colorado Island, Panama. Biotropica 16:125-131.

Lindsay, J. 2016. Whitebox GAT: A case study in geomorphometric analysis. Computers & Geosciences 95:75-84.

Lituma, Christopher M., and David A. Buehler. 2016. Minimal bias in surveys of grassland birds from roadsides. *The Condor: Ornithological Applications* 118(4) : 715-727.

Martinuzzi, S., L. A. Vierling, W. A. Gould, M. J. Falkowski, J. S. Evans, A. T. Hudak, and K. T. Vierling. 2009a. Mapping snags and understory shrubs for a LiDAR-based assessment of wildlife habitat suitability. Remote Sensing of Environment 113:2533-2546.

Martinuzzi, S., L. A. Vierling, W. A. Gould, and K. T. Vierling. 2009b. Improving the characterization and mapping of wildlife habitats with lidar data: Measurement priorities for the inland northwest, USA. Gap Analysis Bulletin 16:1-8.

Mazerolle, M. J. 2023. Version R package version 2.3.3.

McCaffery, R., J. J. Nowak, and P. M. Lukacs. 2016. Improved analysis of lek count data using N-mixture models. The Journal of Wildlife Management 80:1011-1021.

McNair, D. B. 2019. Swainson's Warbler breeding distribution and habitat characteristics in bottomland hardwood forests of the Lower Piedmont in North Carolina: Importance of Chinese Privet. Southeastern Naturalist 18:510-524.

McNeil, D. J., G. Fisher, C. J. Fiss, A. J. Elmore, M. C. Fitzpatrick, J. W. Atkins, J. Cohen, and J. L. Larkin. 2023. Using aerial LiDAR to assess regional availability of potential habitat for a conservation dependent forest bird. Forest Ecology and Management 540:121002.

Meanley, B. 1971. Natural history of the Swainson's Warbler. North American fauna series No. 69. U.S. Department of the Interior, Washington, D.C.

Monk, C. D., D. T. McGinty, and F. P. Day Jr. 1985. The ecological importance of Kalmia latifolia and Rhododendron maximum in the deciduous forest of the southern Appalachians. Bulletin of the Torrey Botanical Club 122:187-193.

Nichols, J. D. 2014. The role of abundance estimates in conservation decision-making. Pages 117-131 *in*: Verdade L., Lyra-Jorge M., Piña C., Applied ecology and human dimensions in biological conservation. Springer. Berlin, Heidelberg

Nicholson, C. P. 1998. Atlas of the breeding birds of Tennessee. The University of Tennessee Press, Knoxville.

Pebesma, E., and R. S. Bivand. 2005. Classes and methods for spatial data: the sp package. R News 5:9-13.

Peters, K. A., R. A. Lancia, and J. A. Gerwin. 2005. Swainson's Warbler habitat selection in a managed bottomland hardwood forest. The Journal of Wildlife Management 69:409-417.

Ralph, C. J., S. Droege, and J. R. Sauer. 1995. Managing and monitoring birds using point counts: standards and applications. Pages 161-168 In: Ralph, C. J., J. R. Sauer,and S. Droege, editors. Monitoring bird populations by point counts. U.S. Department of Agriculture, Forest Service, Pacific Southwest Research Station General Technical Report PSW-GTR-149. Albany, CA.

Roussel, J.-R., D. Auty, N. C. Coops, P. Tompalski, T. R. Goodbody, A. S. Meador, J.-F. Bourdon, F. De Boissieu, and A. Achim. 2020. lidR: An R package for analysis of Airborne Laser Scanning (ALS) data. Remote Sensing of Environment 251:112061.

Roussel, J.-R., D. Auty, F. De Boissieu, A. S. Meador, and B. Jean. 2024. Package 'lidR'.

Royle, J. A. 2004. N-mixture models for estimating population size from spatially replicated counts. Biometrics 60:108-115.

Shanley, C. S., D. R. Eacker, C. P. Reynolds, B. M. Bennetsen, and S. L. Gilbert. 2021. Using LiDAR and Random Forest to improve deer habitat models in a managed forest landscape. Forest Ecology and Management 499:119580.

Sims, E., and W. DeGarmo. 1948. A study of Swainson's Warbler in West Virginia. Redstart 16:1-8.

Smith, E. P. 2002. BACI design. Encyclopedia of Environmetrics 1:141–148.

Somershoe, S. G., S. P. Hudman, and C. R. Chandler. 2003. Habitat use by Swainson's warblers in a managed bottomland forest. The Wilson Bulletin 115:148-154.

Thogmartin, W. E. 2010. Modeling and mapping Golden-winged Warbler abundance to improve regional conservation strategies. Avian Conservation and Ecology 5:12. http://www.ace-eco.org/vol5/iss2/art12

Thomas, B. G., E. P. Wiggers, and R. L. Clawson. 1996. Habitat selection and breeding status of Swainson's warblers in southern Missouri. The Journal of Wildlife Management:611-616.

Twedt, D. J., R. R. Wilson, and A. S. Keister. 2007. Spatial models of northern bobwhite populations for conservation planning. The Journal of Wildlife Management 71:1808-1818.

Vierling, L. A., K. T. Vierling, P. Adam, and A. T. Hudak. 2013. Using satellite and airborne LiDAR to model woodpecker habitat occupancy at the landscape scale. PloS one 8:e80988.

Williams, T. M., D. J. Lipscomb, and C. J. Post. 2004. Defining streamside management zones or riparian buffers. In: Connor K.F. Proceedings of the 12th biennial southern silvicultural research conference (pp. 378-383)

Wu, Q., and A. Brown. 2022. whitebox:"WhiteboxTools" R frontend. R package version 2.

Zhang, M.-G., Z.-K. Zhou, W.-Y. Chen, J. F. Slik, C. H. Cannon, and N. Raes. 2012. Using species distribution modeling to improve conservation and land use planning of Yunnan, China. Biological Conservation 153:257-264.

Ziolkowski, D., M. Lutmerding, W. B. English, V. I. Aponte, and M.-A. R. Hudson. 2023. North American Breeding Bird Survey dataset 1966 - 2022: U.S. Geological Survey, https://www.usgs.gov/data/2023-release-north-american-breeding-bird-survey-dataset-1966-2022#:~:text=The%201966%2D2022%20North%20American,%2C%20and%20unidentified%20species%20groupings).

Appendix

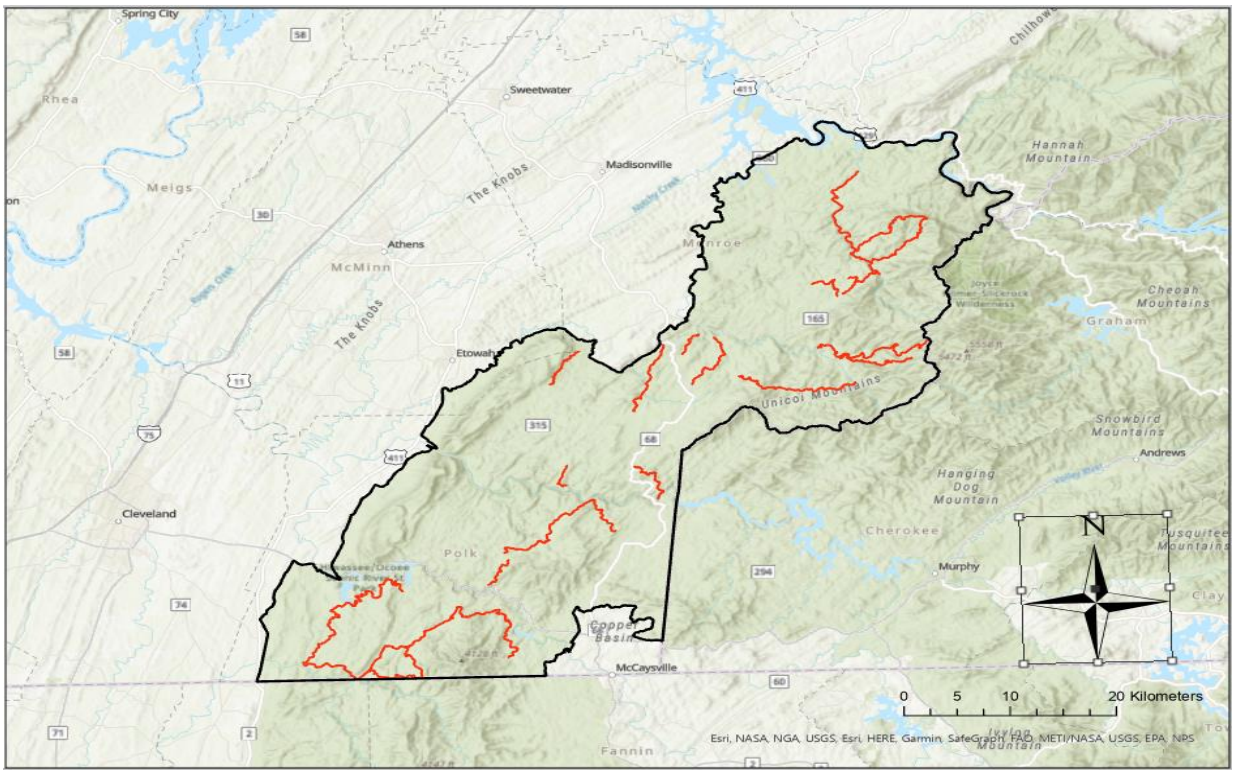

Figure 3.1. Swainson's Warblers roadside survey routes (red), Cherokee National Forest-southern districts, Tennessee, 2022-2023.

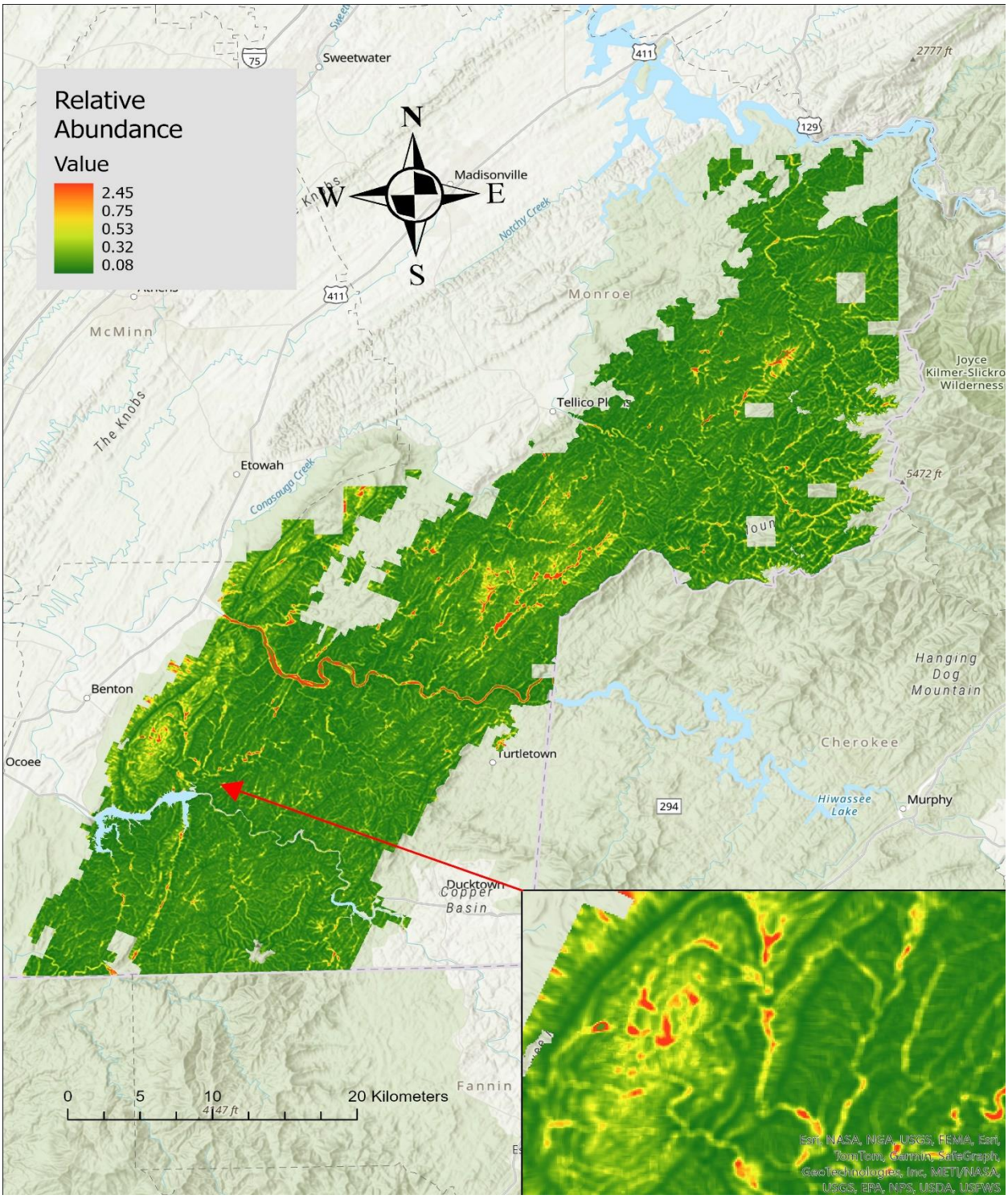

Figure 3.2. Swainson's Warblers relative abundance (birds per point), based on a predictive model using LIDAR-derived covariates, Cherokee National Forest- southern districts, Tennessee, 2022-2023.

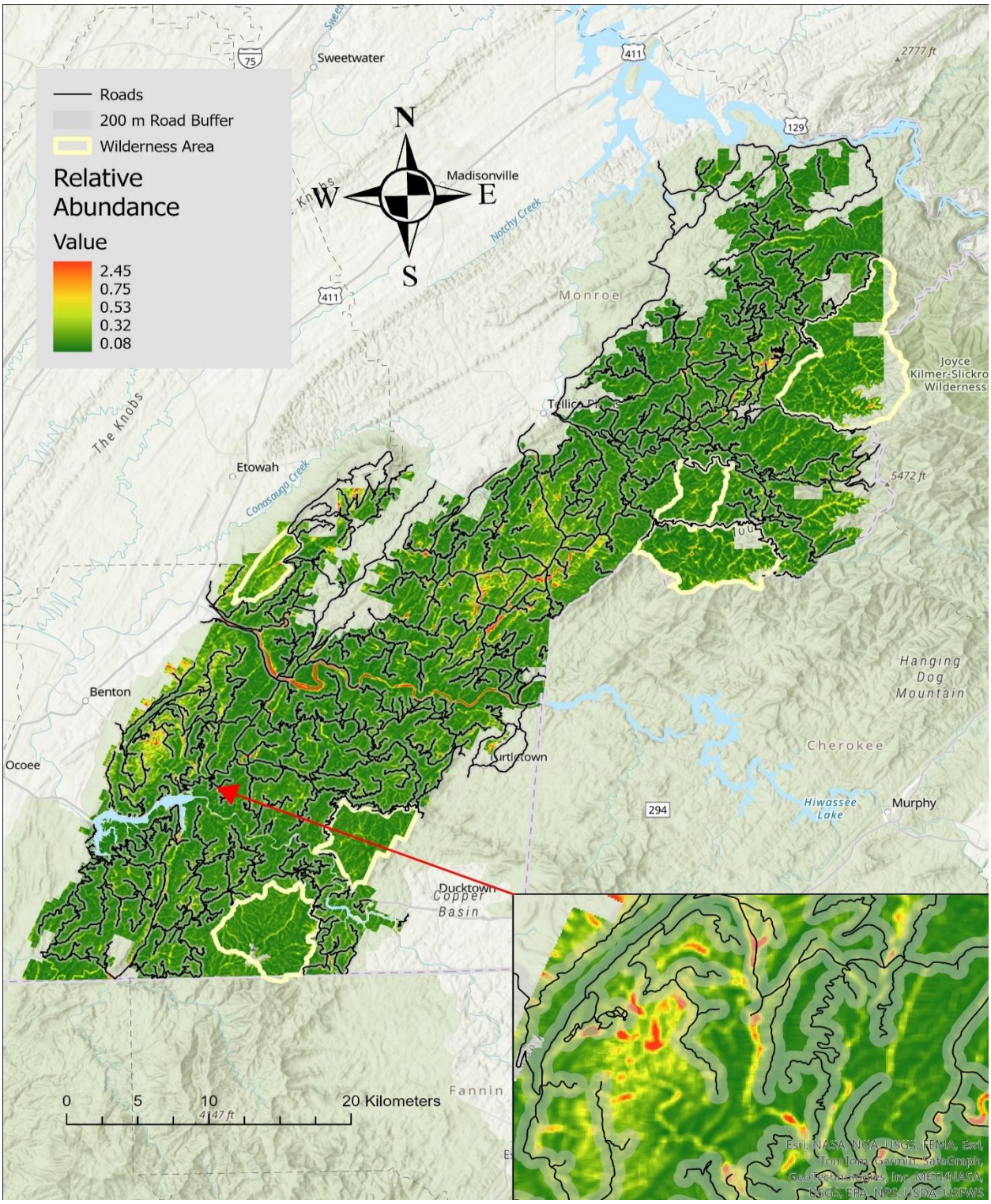

Figure 3.3. Accessibility of Swainson's Warbler relative abundance hotspots by roads, based on a predictive model using Lidar Covariates. Cherokee National Forest- southern districts, Tennessee, 2022-2023.

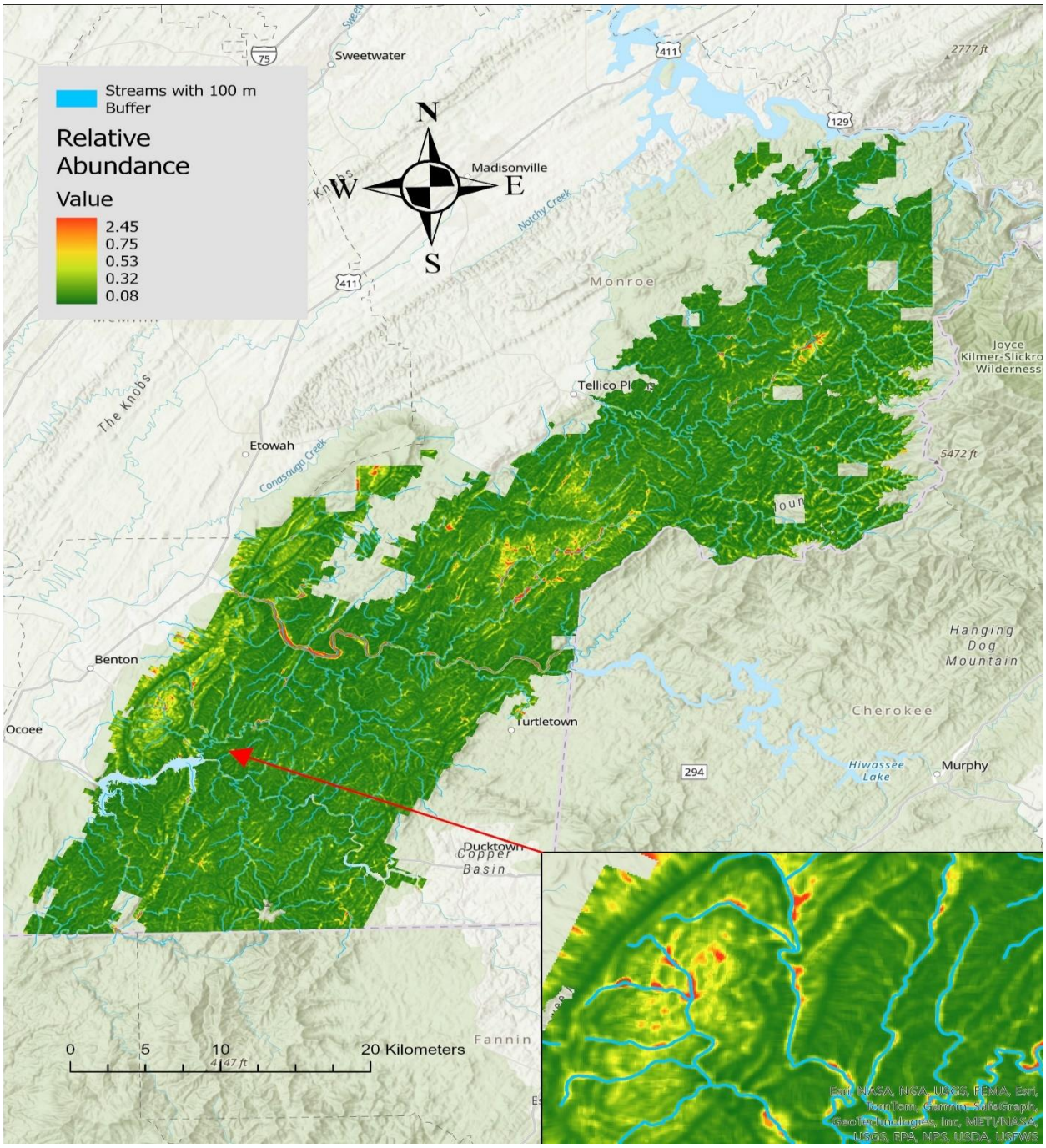

Figure 3.4. Swainson's Warblers relative abundance adjacent to streams and rivers, based on a predictive model using LIDAR covariates Cherokee National Forest- southern districts, Tennessee, 2022-2023.

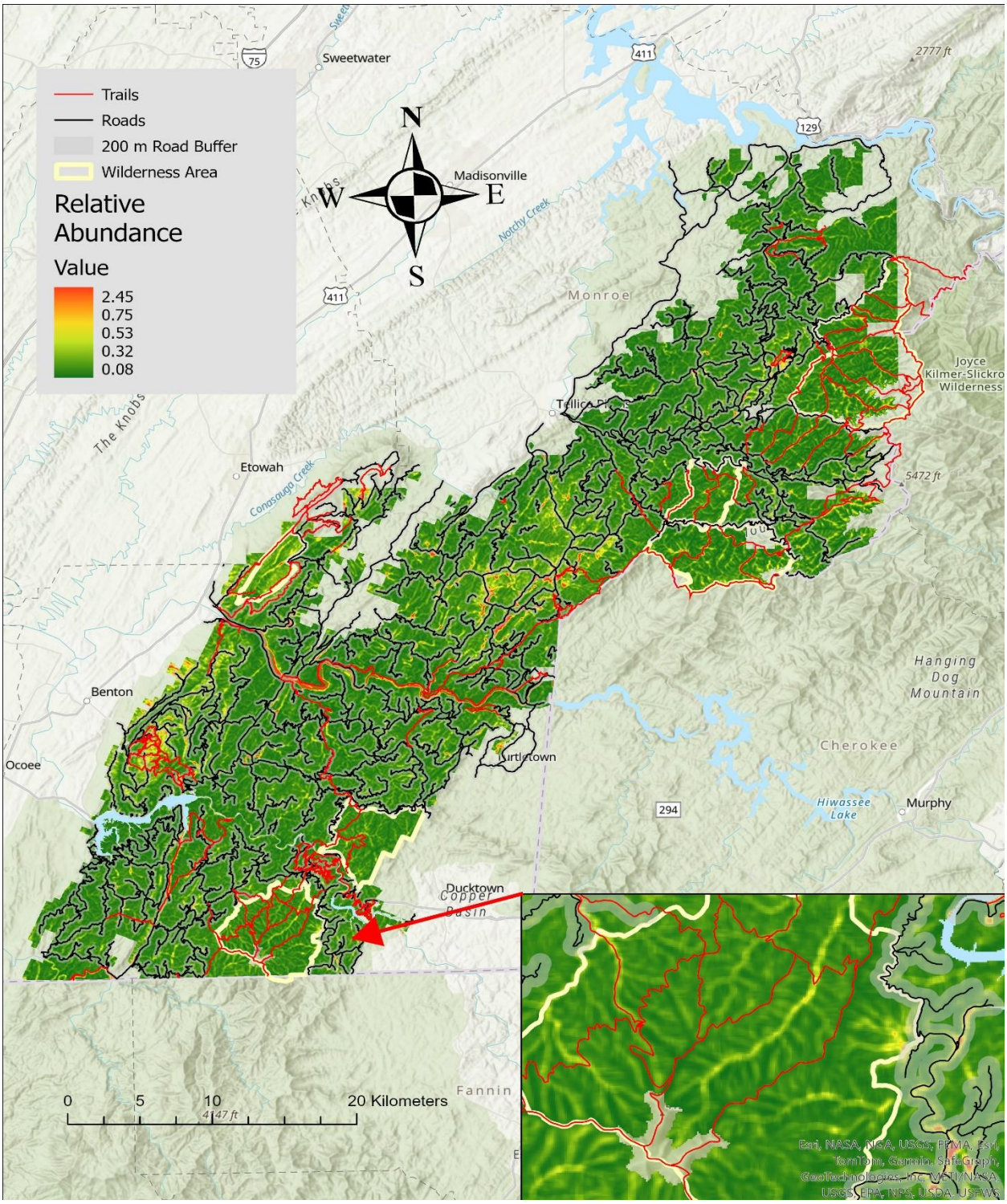

Figure 3.5. Accessibility of Swainson's Warbler abundance hotspots by roads (black) and trails (red), based on a predictive model using LiDAR covariates Cherokee National Forest- southern districts, Tennessee, 2022-2023. Designated Wilderness Areas are outlined in yellow.

Table 3.1 Name, units, equations used for calculation, and a description of variables used to model Swainson's Warbler relative abundance, southern districts of Cherokee National Forest, Tennessee, 2022-2023.

Variable	Full Name	Units	Equation	Description
MedianAngle	Median scan angle	Degrees		Within grain median scan angle
MeanAngle	Mean scan angle	Degrees	$MeanAngle = \overline{\theta}$	Within grain average scan angle
MaxAngle	Maximum scan angle	Degrees		Within grain maximum scan angle
NoPoints	Number of points	Integer count		Number of points within the grain
IQR	Interquartile range	Meters	$IQR = Q_3 - Q_1$	IQR is the range between the third (Q_3) and first quartile (Q_1)
VCI	Vertical complexity index	Unitless, 0-1	$VCI = \left(-\sum_{i=1}^{HB}[(\rho_i \ln(\rho_i))]\right) / \ln(HB)$	VCI is a complexity index calculated using the distribution of lidar returns across equally sized height bins. *HB* is the total number of height bins, and p_i is the proportional abundance of lidar returns in height bin *I* (van Ewijk et al. 2011)
Entropy		Unitless, 01		

Table 3.1 (cont.)

Variable	Full Name	Units	Equation	Description
FHD		Unitless		
VDR	Vertical distribution ratio		$VDR = (H_{Max} - H_{Median})/H_{Max}$	Vertical Distribution Ratio (Goetz et al., 2007)
Rugosity	Rugosity	Meters	$R_T = \sigma(R_{First})$	Rugosity, or top rugosity, is the standard deviation of first returns within the grain (Parker et al. 2004; Atkins et al. 2018)
MOCH	Mean outer canopy height	Meters	$MOCH = \overline{R_{First}}$	Mean outer canopy height as the mean of the first returns per pixel
Skewness	Skewness	Unitless	$Skewness = \left(3 \times \left(\frac{Mean(z) - Median\ (z)}{\sigma(z)}\right)\right)$	A measure of the asymmetry of lidar point return distribution.
FirstBelow$_z$	First returns below z	Percentage	$Below_z = \frac{\sum R_{First} < z}{\sum R_{First}} \times 100$	Percentage of first returns below a specific height (z, meters)
Below$_z$	Returns below x	Percentage	$Below_z = \frac{\sum z < z}{\sum z} \times 100$	Percentage of all returns below a specific height (z, meters)

Table 3.1 (cont.)

Variable	Full Name	Units	Equation	Description
*p*10 … *p*95	Percentile heights	Meters	$(\mathrm{p}_x = \mathrm{mode}[\mathrm{F}(\mathrm{x}_\mathrm{k})])$	Height (m) at which there are X percent of returns below (i.e., p95 of 10 m indicates 95% of the returns are below this height for a given pixel.
isd	Standard deviation of intensity	Unitless		SD of lidar return intensity per pixel.
imean	Mean intensity	Unitless		Mean of lidar return intensity per pixel
DISTANCE_ TO_WATER	Distance to nearest water body	Meter		Calculated in ArcGIS Pro, using the near function.
ASPECT		Categorized Aspect	Degrees	Direction of slope face. Categorized into bins established by ArcGIS pro.
SLOPE	Hill Slope	Degrees		Steepness of terrain.

Table 3.2. Bootstrap analysis output for the best-performing Swainson's Warbler N-mixture model, southern districts of Cherokee National Forest, Tennessee, 2022-2023.

Parametric Bootstrap Statistics:

	t0	mean(t0 - t_B)	StdDev(t0 - t_B)	Pr(t_B > t0)
SSE	196	-7.918	25.6	0.605
Chisq	659	-74.537	58.8	0.922
freemanTukey	183	0.431	12.7	0.495

t_B quantiles:	0.0%	2.5%	25.0%	50.0%	75.0%	97.5%	100.0%
SSE	133	158	186	204	219	257	312
Chisq	591	635	692	728	769	865	1027
freemanTukey	147	157	174	182	191	206	228

t0 = Original statistic computed from data

t_B = Vector of bootstrap samples

Chapter 4: Conclusion

We used on-the-ground and remotely-sensed habitat variables to conduct the first major analysis of Swainson's Warbler territory selection, a species of conservation concern in Tennessee. We successfully modeled the distribution and amount of potential habitat for this species on the southern ranger districts of the Cherokee National Forest.

Key Findings:

- Percent understory cover, visual obstruction, percent canopy cover, rhododendron presence, and slope were significant predictors of Swainson's Warbler territory selection.
- Remotely-sensed variables (topographic wetness index, percent of first returns below 2 m) can be successfully used to predict SWWA territory selection, but were not as strongly related to SWWA territory selection as on-the-ground covariates.
- Although the plant species Swainson's Warblers utilize in the Appalachian Mountains differ from the plant species used in the Coastal Plain, the drivers of territory selection are similar; understory vegetation density, canopy cover, slope, and soil moisture.
- We successfully modeled Swainson's Warbler relative abundance using four remotely-sensed variables: topographic wetness index, mean outer canopy height, percent of first returns below 1 m, and slope.
- The southern ranger districts of the Cherokee National Forest had ~3,500 ha of potential SWWA habitat in 2022 – 2023.
- Fifty-five% of potential habitat was within 200 m of roads. A roadside-based monitoring strategy with 5-min point counts with playback could effectively monitor SWWA populations on the Cherokee National Forest.
- Five% of potential habitat was located within less accessible wilderness areas that could be accessed via foot trails for monitoring SWWA and other priority bird populations.
- An estimated 26% of potential habitat was located within 30 m of streams and thus was regulated by current U.S. Forest Service streamside management zone guidelines.

Vita

Dawson Rader is from Bean Station, Tennessee. He grew up outside exploring Cherokee lake, forming a passion for the outdoors. He obtained a Bachelor's of Science in Wildlife and Fisheries Management from the University of Tennessee, Knoxville in 2022. While at the University of Tennessee he was heavily involved with the Student Chapter of The Wildlife Society and worked with Golden-winged Warblers at North Cumberland WMA and Northern Bobwhite at Kyker Bottoms WMA. These positions helped him to form a passion for imperiled bird species and their management. After he graduated with his Bachelor's degree, he transitioned into a Masters position at his alma mater; pursuing Master of Science degree where he studied the habitat and distribution of the Swainson's Warbler.